Title
Contrasting mechanisms of penile urethral formation in mouse and human.

Authors
Liu, Ge
Liu, Xin
Shen, Joel
et al.

Publication Date
2018-05-01

DOI
10.1016/j.diff.2018.05.001

Peer reviewed

Differentiation 101 (2018) 46–64

Contents lists available at ScienceDirect

Differentiation

journal homepage: www.elsevier.com/locate/diff

Contrasting mechanisms of penile urethral formation in mouse and human

Ge Liu[a,b], Xin Liu[a,b], Joel Shen[b], Adriane Sinclair[b], Laurence Baskin[b], Gerald R. Cunha[b,*]

[a] Department of Pediatric Surgery, Shengjing Hospital of China Medical University, Shenyang, Liaoning, China
[b] Department of Urology, University of California, San Francisco, CA, United States

ARTICLE INFO

Keywords:
Urethra
Penis
Prepuce
Hypospadias
Genital tubercle
External genitalia

ABSTRACT

This paper addresses the developmental mechanisms of formation of the mouse and human penile urethra and the possibility that two disparate mechanisms are at play. It has been suggested that the entire penile urethra of the mouse forms via direct canalization of the endodermal urethral plate. While this mechanism surely accounts for development of the proximal portion of the mouse penile urethra, we suggest that the distal portion of the mouse penile urethra forms via a series of epithelial fusion events. Through review of the recent literature in combination with new data, it is unlikely that the entire mouse urethra is formed from the endodermal urethral plate due in part to the fact that from E14 onward the urethral plate is not present in the distal aspect of the genital tubercle. Formation of the distal portion of the mouse urethra receives substantial contribution from the preputial swellings that form the preputial-urethral groove and subsequently the preputial-urethral canal, the later of which is subdivided by a fusion event to form the distal portion of the mouse penile urethra. Examination of human penile development also reveals comparable dual morphogenetic mechanisms. However, in the case of human, direct canalization of the urethral plate occurs in the glans, while fusion events are involved in formation of the urethra within the penile shaft, a pattern exactly opposite to that of the mouse. The highest incidence of hypospadias in humans occurs at the junction of these two different developmental mechanisms. The relevance of the mouse as a model of human hypospadias is discussed.

1. Introduction

Formation of the penile urethra has been studied in rodents with the tacit, but unproven, assumption that developmental processes in rodent models are relevant to human penile development. Clearly there are some developmental events shared between species such as the formation of a solid urethra plate within the embryonic genital tubercle (GT), which is observed in mouse, rat, rabbit, tamar wallaby, spotted hyena and human (Armfield et al., 2016; Li et al., 2015; Hynes and Fraher, 2004a; Kluth et al., 2011; Agras et al., 2006, 2007b, 2007a; Cunha et al., 2014; Butler et al., 1999; Kurzrock et al., 2000). Most of the mouse penile urethra forms by direct canalization of the urethral plate (Hynes and Fraher, 2004a, 2004b; Seifert et al., 2008). We have suggested that the distal portion of the mouse penile urethra, including the urethral meatus, develops via multiple fusion events (Baskin et al., 2001; Sinclair et al., 2016a). This idea regarding formation of the distal portion of the mouse penile urethra has emerged through a focused anatomical analysis of the developing and adult mouse penile urethra and has been dealt with superficially in a series of recent papers (Sinclair et al., 2016b, 2016a; Yang et al., 2010; Mahawong et al., 2014a, 2014b; Blaschko et al., 2013). In this paper this idea is pursued through review of previous studies augmented with additional new observations.

Human penile urethral development occurs via a radically different process that starts with the formation of the solid urethral plate, which extends into the developing glans. The urethral plate within the developing penile shaft canalizes to form an open diamond-shaped urethral groove whose edges (urethral folds) subsequently fuse in the midline in a proximal to distal direction to form the penile urethra (Li et al., 2015; Shen et al., 2016). This process of urethral groove formation and subsequent urethral fold fusion forms the human penile urethra within the penile shaft. However, scanning electron micrographs demonstrate that the urethral groove does not extend into the glans suggesting that formation of the human glandar urethra might occur via a substantially different developmental process (Li et al., 2015; Shen et al., 2016).

The goal of this paper is to explore the morphogenetic mechanisms of penile urethral development in mice and humans from the perspec-

Abbreviations: MUMP, male urogenital mating protuberance; E, embryonic; P, postnatal; K, keratin; GT, genital tubercle; OPT, optical projection tomography; PUG, preputial-urethral groove; PUC, preputial-urethral canal; VPG, ventral penile groove; AR, androgen receptor

* Corresponding author.
E-mail address: gerald.cunha@ucsf.edu (G.R. Cunha).

https://doi.org/10.1016/j.diff.2018.05.001
Received 5 March 2018; Received in revised form 14 May 2018; Accepted 15 May 2018
Available online 17 May 2018

Table 1
Antibodies used in this study.

Antibody	Source	Catalogue #	Concentration
Keratin 6	Acris Antibodies	AM21068PU-S	1/200
Keratin 7	E.B. Lane[a]	LP1K	1/10
Keratin 8	E.B. Lane[a]	LE41	1/10
Keratin 10	Dako	M7002	1/50
Keratin 14	BioGenex	LL002	1/100
Keratin 19	E.B. Lane[a]	LP2K	1/10
Uroplakin1	T. T. Sun[b]		1/100
Foxa1	Atlas Antibodies	HPA050505	1/500
Androgen receptor	Genetex	GTX62599	1/100

[a] Institute of Medical Biology, Singapore.
[b] New York University, New York.

Table 2
List of human specimens.

Code	Heel-Toe (mm)	Age (weeks)
AC324	13.5	13
AC560	14	14
AC302	15.3	15
AC280	16.0	16
AC416	17.0	17

tive of: (a) direct canalization of the urethral plate and (b) epithelial fusion events. Our studies suggest but that in these two species both morphogenetic mechanisms occur, but in different proximal-distal regions of the developing penis. Accordingly, the relevance of mouse penile development as a model relevant to human penile development will be discussed.

2. Materials and methods

2.1. Mouse studies

The University of California, San Francisco (UCSF) Institutional Animal Care and Use Committee approved all animal protocols. Timed-pregnant CD-1 mice (Charles River Breeding Laboratories, Wilmington, MA, USA) were housed in polycarbonate cages ($20 \times 25 \times 47\ cm^3$) with laboratory-grade pellet bedding in the UCSF Pathogen Specific Barrier housing facility. The mice were given Purina lab diet (#5058) and tap water ad libitum. They were acclimated to 20° to 23 °C and 40–50% humidity on a schedule of 14 h light and 10 h dark. Embryos and neonates were collected at the following ages: embryonic days 14, 15, 16, 17, and 18/birth. At least 3 mice were used for each time point. Additional mice at these time points were used for immunohistochemical studies. Accordingly this paper is based upon analysis of 45 mice.

External genitalia were dissected and photographed using a digital camera, and were then fixed in 10% buffered formalin. Samples were paraffin embedded and serially sectioned at 7 μm for histological staining with hematoxylin and eosin (H & E). Immunohistochemistry (IHC) was carried out as previously described (Rodriguez et al., 2012) on sections of mouse and human external genitalia using the antibodies indicated in Table 1. Signal detection was achieved using either the Vector ABC System (Vector Laboratories, Foster City, CA, USA) followed by exposure to diaminobenzidine (Sigma®). Alternatively, immunoflourescent detection was carried out following incubation with goat anti-rabbit fluorophore-conjugated secondary antibodies (diluted 1:500, Abcam) for 1 h at room temperature. Sections exposed to all steps except the application of the primary antibodies were used as negative controls.

Metrics of pertinent key morphological features were obtained by counting the number of serial transverse sections from the first section of the distal tip of the GT to the solid or canalized urethral plate (urethra). Actual distances were converted to microns from the distal

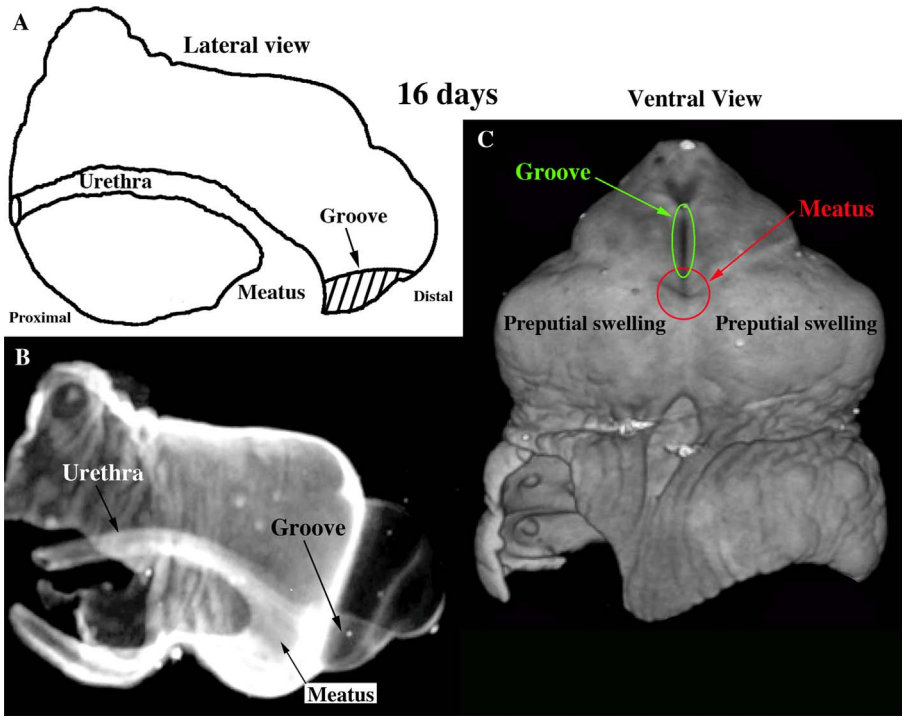

Fig. 1. Diagrammatic (A) and optical projection tomography (OPT) images of the E16-day embryonic genital tubercle. Image (B) is a semi-transparent lateral view of an E16-day external genitalia stained with an antibody to E-cadherin in which the canalized urethral plate (urethra) can be seen opening to the exterior into a groove a considerable distance from the distal tip of the GT. (A) is a diagrammatic representation of (B). (C) is an ventral OPT surface rendering of specimen (B) in which the urethral meatus and ventral penile groove can be seen. Modified from Sinclair et al. (2016b) with permission.

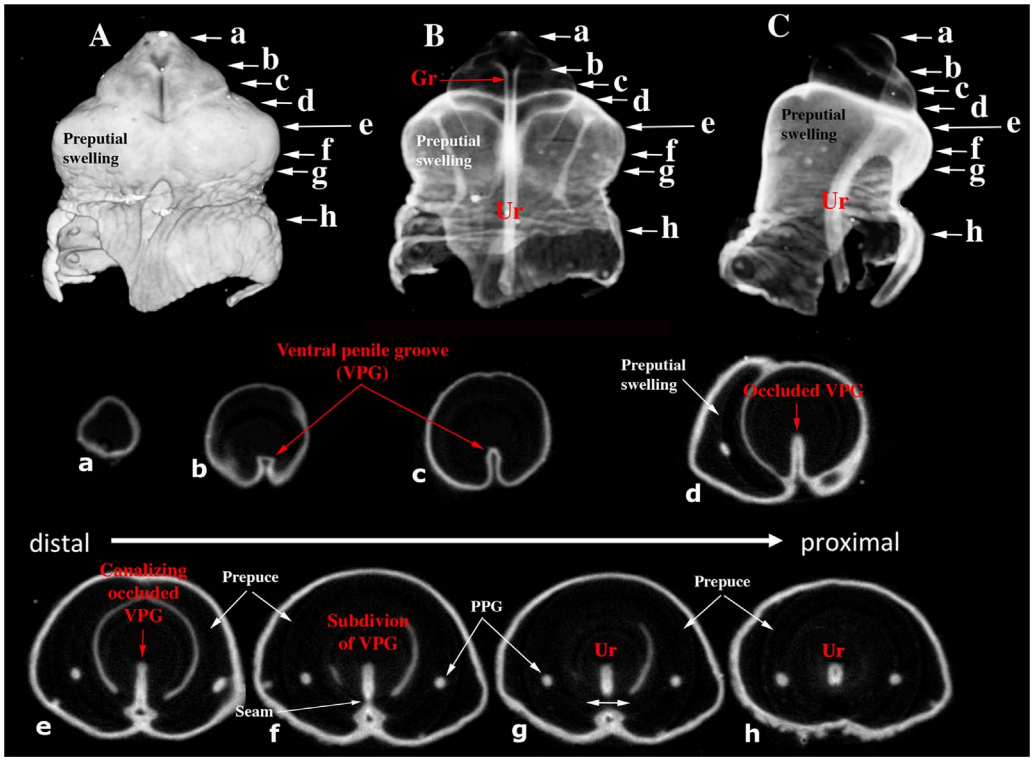

Fig. 2. Optical projection tomography wholemount images of a 16-day embryonic genital tubercle stained with antibody to E-cadherin (A-C). (A) is a ventral surface rendering. (B) is a semi-transparent ventral-dorsal image showing the urethra (Ur) and the ventral penile groove (Gr). Lower case letters (a-h) in images indicate the positions of the OPT sections illustrating the ventral penile groove (VPG), the occluded ventral groove (Occluded VPG), the canalizing occluded VPG, subdivision of the occluded VPG and the urethra (Ur). In (f & g) the epithelial seam is being eliminated to establish midline mesenchymal confluence (double-headed arrow) and establishing a "Stand-alone" urethra. PPG= preputial gland. Modified from Sinclair et al. (2016b) with permission.

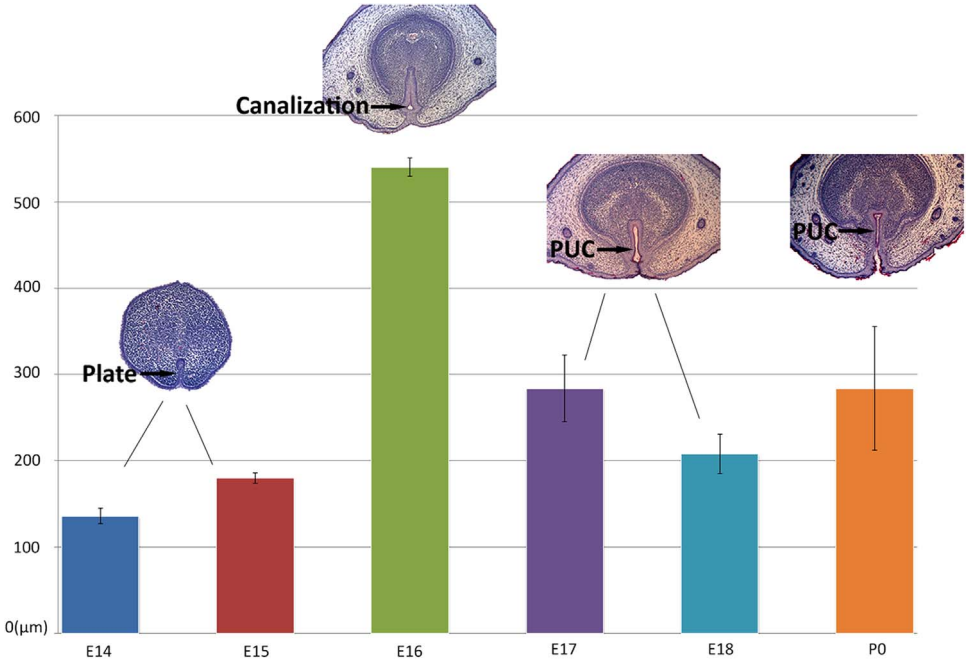

Fig. 3. A chart depicting the distance from the distal tip of the genital tubercle to the distal extremity of solid (E14 & E15) urethral plate, to the distal extremity of the canalized urethral plate (E16), and to the distal extremity of the preputial-urethral canal (PUC) (E17-P0). Histologic sections illustrate the type of structure. The closest structure to the tip of the genital tubercle is the solid urethral plate at E14, which is ~130 μm from the tip of the genital tubercle. The data represent the average of 3–5 specimens per age.

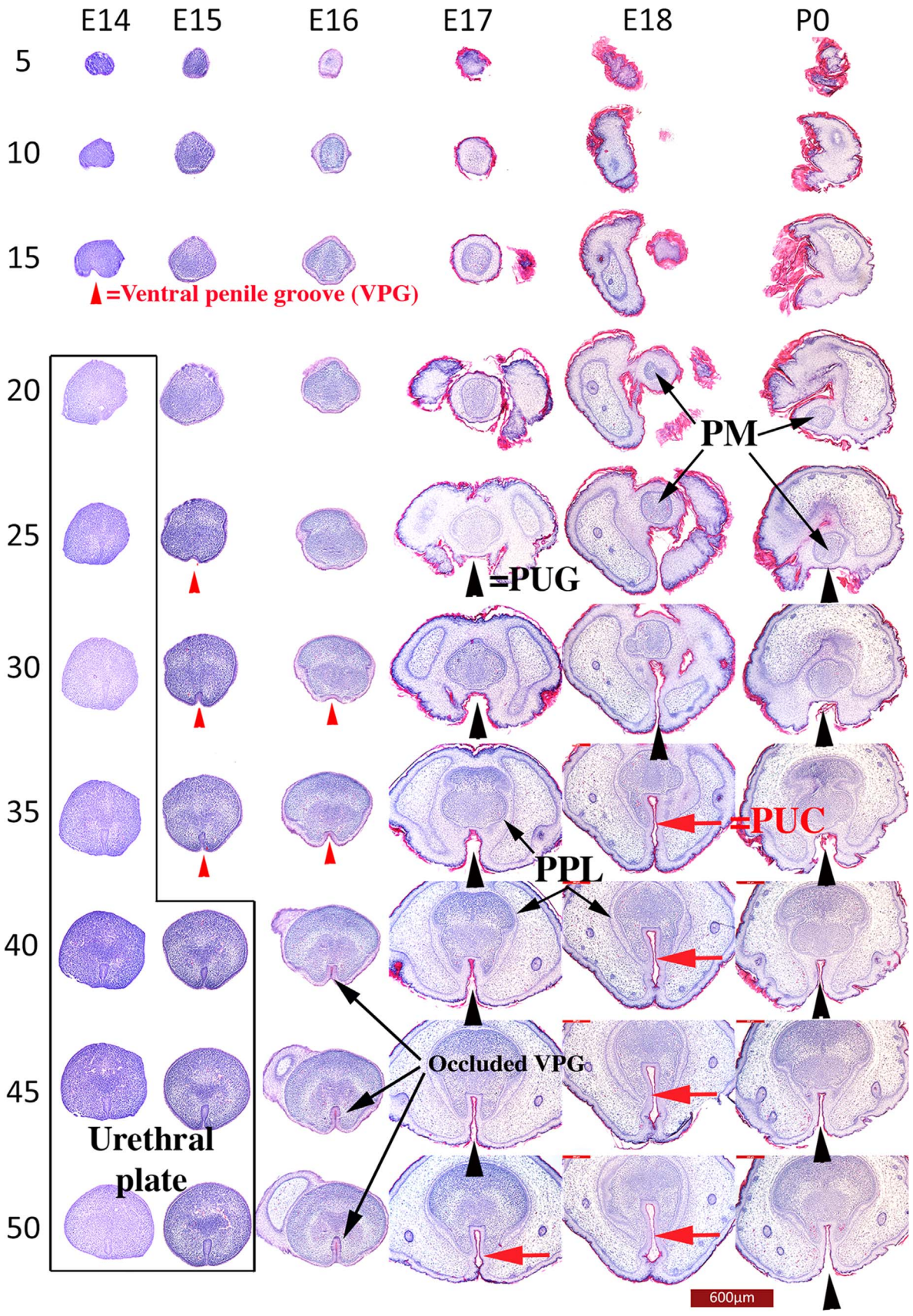
E14
E15
E16
E17
E18
P0
5
10
15
20
25
30
35
40
45
50
=Ventral penile groove (VPG)
PM
=PUG
=PUC
PPL
Occluded VPG
Urethral plate
600μm

Fig. 4. Serial histologic sections 5–50 of mouse external genitalia from E14 to P0 male mice. Sections are 7 μm in thickness. Section numbers on the left are indicative of distance from the distal tip of the GT. At 14 days that the solid urethral plate is first seen at section 20 and that the ventral penile groove is seen at section 15. At 15 days the ventral penile groove is first seen at section 25, and the solid urethral plate is first seen at section 40. Note the absence of preputial swellings in the E14 and E15 specimens. At 16 days a shallow groove is first seen at section 30, which deepens and becomes occluded through sections 40–50. Note also the appearance of the left preputial swelling at section 45. At 17 days the preputial-urethral groove (PUG) is seen in sections Section 25–45. Ventral fusion of the PUG occurs at section 50 (red arrow). At E16 and E17 the dense centrally located penile mesenchyme is separated from loose preputial mesenchyme by the preputial lamina (PPL), and at E17 the preputial swellings are first encountered at section 20, which become more prominent in deeper sections. At 18 days a fully formed preputial-urethral groove is seen at section 30, whose edges are fusing to form the preputial-urethral canal (section 35, PUC, green arrows). At birth (P0) due to the distal expansion of the preputial swellings, initial sections (5–15) only contain preputial tissue. Centrally placed dense penile mesenchyme (PM) is first seen at section 20 and persists thereafter. The preputial-urethral groove (PUG) is first encountered at section 25 and narrows and deepens in subsequent sections (30–50). (For interpretation of the references to color in this figure legend, the reader is referred to the web version of this article.)

GT tip. Statistical analysis of distance was done using Student's t-tests. A $p < 0.05$ was considered significant. Data are expressed as mean ± SE.

2.2. Human studies

Human fetal specimens were collected free of patient identifiers after elective termination of pregnancy (Committee on Human Research, University of California, San Francisco, IRB# 12-08813) (Table 2). Male gender was confirmed by Wolffian (mesonephric) duct morphology and the gross presence of prostate. Since all aborted specimens were disrupted by the surgical procedure, heel-toe length proved to be the only useful determinant of gestational age (Drey et al., 2005; Mercer et al., 1987; Mhaskar et al., 1989). Human male external genitalia were sectioned serially and stained with H & E.

3. Results and discussion

For several years the mechanism of development of the mouse penile urethra has been debated in the literature between our laboratory and Martin Cohn's laboratory. The Cohn position is that “urethral plate is derived from endoderm that gives rise to the entire urethra” (Seifert et al., 2008). We agree that most of the proximal portion of the mouse penile urethra develops from direct canalization of the urethral plate as described previously (Hynes and Fraher, 2004a, 2004b; Seifert et al., 2008), but that the distal portion of the mouse penile urethra develops as a result of epithelial fusion events, which have been annunciated briefly in several previous papers. In this study we present our case for a dual mechanism of mouse (and human) penile urethral development through review of previous observations in combination with new data.

The question of whether the urethral plate gives rise to the entire mouse urethra as suggested by Seifert et al. requires critical assessment of the whether the urethral plate actually extends to the distal tip of the genital tubercle (GT). Seifert et al. state “that the entire urethra, including the distal (glandar) region, is derived from endoderm.” According to Seifert et al., at E15.5 and E17.5 days (Fig. 3, Seifert et al., 2008) LacZ staining extends all the way to the distal tip of the GT. Seifert et al. further state. “Within the distal portion of the glans, which is not yet surrounded by the prepuce, the urethral plate (detected via LacZ staining) remains in contact with the overlying ectoderm (Fig. 3E, F).” Seifert's statements taken together are clear, “the entire urethra, including the distal (glandar) region, is derived from endoderm” (Seifert et al., 2008). However, histologic confirmation of the urethral plate at or near the distal tip of the GT was not provided, and our serial histologic sections clearly demonstrate that the urethral plate does not extend to the distal aspect of the GT as described below. Another important point is that the histologic/immunohistochemical signature of the embryonic urethral plate has not previously been reported and, more important, whether the developing distal portion of the urethra exhibits a similar signature.

3.1. Development of the mouse penile urethra

As stated above, most of the mouse penile urethra occurs via direct canalization of the urethral plate (Hynes and Fraher, 2004a, 2004b; Seifert et al., 2008). Seifert et al. assert that “at E15.5, the urethra extends to the distal tip of the genital tubercle and is composed entirely of cells descended from Shh-GFPcre-expressing endoderm” (Seifert et al., 2008). In contrast, optical projection tomography (OPT) of the 16-day embryonic mouse GT (Sinclair et al., 2016b) demonstrated that the canalized urethral plate does not extend to the distal tip of the mouse GT. Instead, OPT data showed that the canalized urethral plate (the urethra) terminates at 16 days of gestation approximately 1 mm from the distal tip of the GT by opening to the exterior into a groove (which we call the ventral penile groove) that extends distally from the canalized urethral plate (urethra) (Figs. 1 and 2) (Sinclair et al., 2016b). To pursue this further, serial sections were examined from mouse GTs at 14, 15, 16, 17, 18 days of gestation/birth (3 mice per time point). By counting serial sections the distance in microns was calculated from the distal tip of the GT to the beginning of the solid or canalized urethral plate. At all ages studied (E14 to birth) the solid or canalized urethral plate did not extend to the distal tip of the GT (Fig. 3). Clearly, the data from ShhGFPcre;R26R mouse embryos is at odds with the histologic data. The striking lack of correspondence between the histologic and “Shh-LacZ” data coupled with LacZ staining of ectodermal structures (hair follicles and the preputial glands) (Seifert et al., 2008) is a major concern regarding the reliability of the Shh-LacZ method for assessing the endoderm lineage. Serial histologic and OPT sections demonstrate that the distal portion of the GT consists of mesenchyme surrounded by epidermis (Fig. 2a and Fig. 4, E14 sections 5 & 10, E15 sections 5–20, E16 sections 5–25). The first anatomic feature encountered proximal to the distal tip of the GT was the ventral penile groove (red arrowheads Fig. 4, E14 section 15, E15 sections 5–35, E16 sections 30–50 & Fig. 6A). The term “ventral penile groove” is justified as it is a ventral groove exclusively within the male GT, and is not associated with the prepuce (Fig. 2b and c, Fig. 4, E14, E15 & E16). The distance from the distal tip of the GT to the solid or canalized urethral plate varied with gestational age (Fig. 3) and ranged from ~130 to ~540 μm (Fig. 3). The solid urethral plate (Fig. 6B) was observed at 14 and 15 days of gestation as described previously (Seifert et al., 2008; Hynes and Fraher, 2004a) but was located proximal to the ventral penile groove (Fig. 4, E14 sections 20–50, E15 sections 40–50, see boxed area). Canalization of the 14- and 15-day urethral plate was observed in the proximal portion of the GT (Fig. 5, E14 section 100), while distally the urethral plate was solid (Fig. 4, boxed area) as described previously (Seifert et al., 2008; Hynes and Fraher, 2004a). Most important, at 14 days of gestation the solid and canalized embryonic urethral plate (urethra) (see Fig. 5, E14 section 100) was observed proximal to the ventral penile groove and proximal to the tip of the GT (see Fig. 4, E14 section 15). Similar observations are evident at days 15 of gestation (Figs. 4 and 5).

The 16-day GT requires special critical attention. Extending

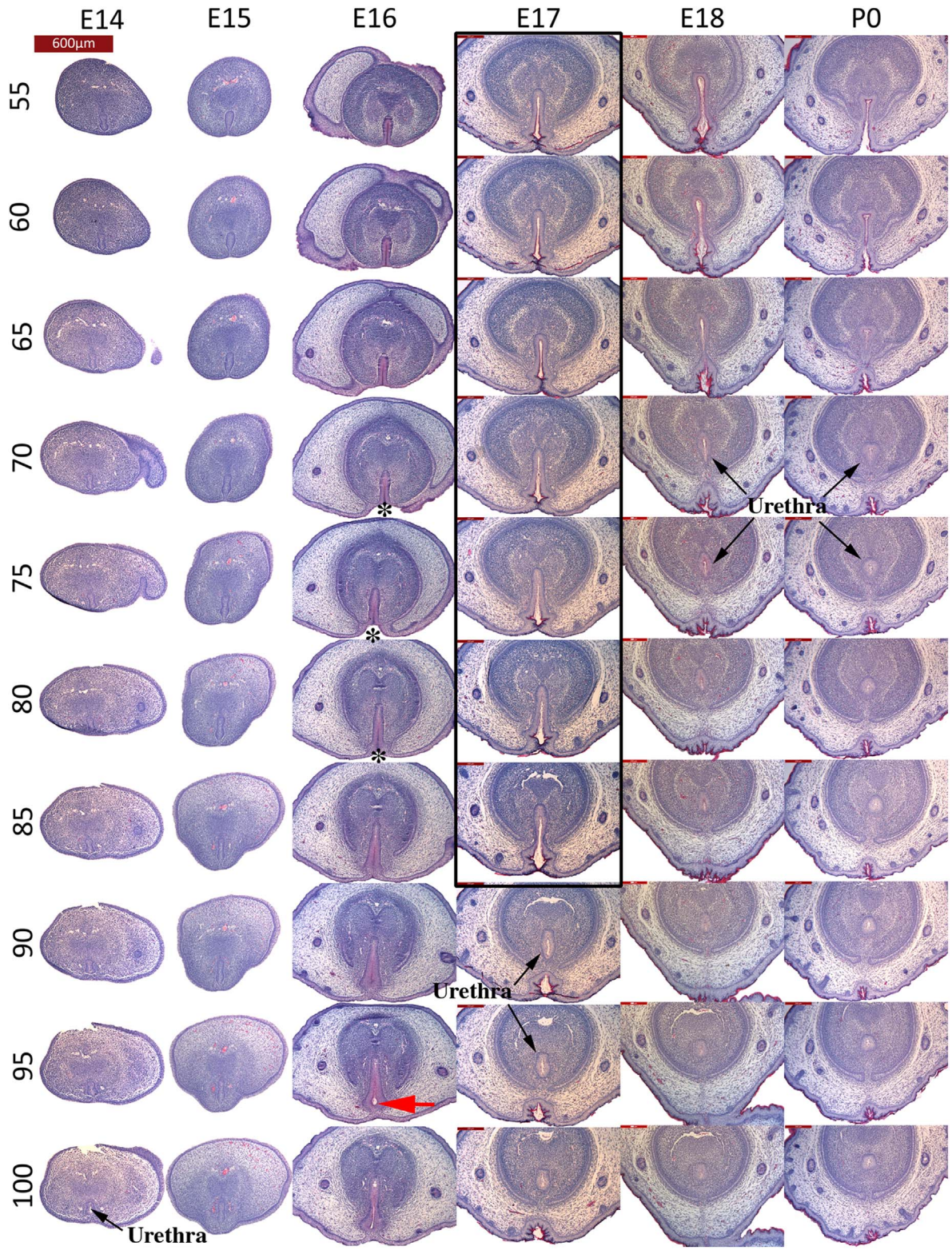

Fig. 5. Serial histologic sections 55–100 of mouse external genitalia from E14 to P0 male mice. Sections are 7 µm in thickness. At 14 and 15 days the solid urethral plate is present and is attached to the epidermis (E14, sections 55–95, E15, sections 55–100). The canalized urethral plate (urethra) is seen at E14 initially at section 100, while at day E15 canalization of the urethral plate occurs at section 130 (not illustrated). At 16 days an occluded urethral groove is seen in sections 55–90 in association with a shallow ventral preputial-urethra groove (asterisks) in sections 70- and 80. At E16 canalization of the occluded urethral groove occurs at section 95 (red arrow) to form the preputial-urethral canal (PUC). At 17 days sections 55–85 (boxed) show the preputial-urethral canal, which at section 90 has been subdivided into the urethra surrounded by dense penile mesenchyme. At birth (P0) the preputial-urethral groove (PUG, section 55) has undergone a fusion event in section 60 creating an epithelial seam (large red arrow) that has disappeared in section 70 resulting in a"stand alone" urethra surrounded by penile mesenchyme seen in all subsequent sections. A higher magnification sequence of the P0 events can be seen in Fig. 11. (For interpretation of the references to color in this figure legend, the reader is referred to the web version of this article.)

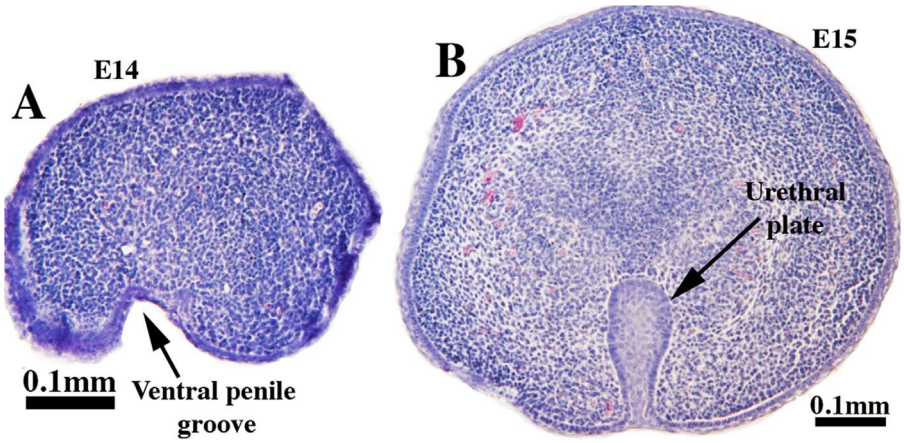

Fig. 6. Transverse sections of an E14 genital tubercle. Section (A) is near the distal GT tip and depicts the ventral penile groove. Section (B) is more proximal and depicts the solid urethral plate.

dorsally from the ventral penile groove at E16 is a solid epithelial plate (Fig. 4, E16, sections 40–50 and Fig. 5 E16, sections 55–90), which superficially resembles the urethral plate seen at 14 and 15 days of gestation. This structure is not the solid urethral plate, but instead is the "occluded ventral penile groove" occluded by squamous epithelial cells lining the original ventral penile groove (Figs. 2d and 7). Position-wise, Fig. 7 corresponds to Fig. 4 E15, sections 40–50 and likewise corresponds to the regions between Fig. 2c-d. Fig. 7 depicts the E15 day solid urethral plate (top) and 3 distal to proximal sections of the occluded ventral penile groove. As can be seen, the histological signature of the occluded ventral penile groove at E16 differs profoundly from that of the definitive urethral plate seen in E14- and E15-day mouse embryos (Figs. 6B and 7). Moreover, the histological signature of the occluded ventral penile groove is virtually identical to that of the epidermis with which it is continuous. Eosinophilic non-nucleated squames are seen both within the occluded ventral penile groove (Fig. 7, arrows) and as well on the apical surface of the adjacent epidermis (Fig. 7, black arrowheads). Higher magnification reveals keratohyalin granules (distinctive of epidermis) (Manabe and O'Guin, 1992) centrally situated within the occluded ventral penile groove (not illustrated), suggesting that the ventral penile groove and the occluded ventral penile groove are derived from epidermis. Such features are not seen in the definitive urethral plate of 14- and 15-day mouse embryos (compare Figs. 6B and 7). The occluded PUG is seen only at 16 days of gestation and subsequently canalizes to created a lumen (Fig. 2e and Fig. 5 E16, section 95, large red arrow),

At 16 days of gestation and thereafter the preputial swellings grow distally to eventually cover the developing GT (Baskin et al., 2002). During this process the preputial swellings converge and fuse in the ventral midline (Fig. 8) (Perriton et al., 2002; Petiot et al., 2005). In addition, as the preputial swellings grow distally to eventually completely cover the GT (Figs. 8 and 9), the preputial lamina is laid down (Figs. 9–11). As the preputial swellings approach each other in the midline, a ventral groove is formed which is called the "preputial-urethral groove" (PUG) (Fig. 4, large black arrowheads and Fig. 10D). The edges of the PUG fuse to form the preputial-urethral canal (PUC) (Fig. 4, red arrows and Figs. 10E, 11D). The PUG is continuous laterally with the epidermis of the preputial swellings and accordingly has a histologic signature virtually identical to that of the epidermis (Figs. 10D and 11). The histologic signature of the PUC (following fusion of the edges of the PUG) is also similar to that of epidermis (Figs. 10D and 11E & F), especially the ventral portion of the PUG and PUC where cornified squames can be seen (Fig. 10E & F, red arrows).

During the course of penile urethral development, it is crucial to use meaningful terminology. Accordingly, the groove seen at 14–15 days of gestation is appropriately called the ventral penile groove, as it is a groove exclusively in the GT (Fig. 6A). At 16 days of gestation and thereafter the shallow surface groove and its dorsal extension occludes with non-nucleated squames and thus the term, the "occluded ventral penile groove" applies (Fig. 7). A ventral groove formed in large part by the preputial swellings as they approach the midline is designated the "preputial-urethral groove (PUG) consistent with the contribution from the preputial swellings and its ultimate fate to form the urethra (Fig. 10). Closure of the PUG via an epithelial fusion event forms the preputial-urethral canal (PUC) (Fig. 10E and Fig. 11D), whose dorsal portion is segregated via a fusion event to form the penile urethra (Figs. 10 and 11). The terms, PUG and PUC, are justified because these two structures are involved in development of both the prepuce and the urethra. In addition, the connective tissue associated with the PUG and PUC are clearly of two types. The stroma associated with the dorsal portion of the PUG and PUC is dense penile stroma and is located internal to the preputial lamina (Figs. 10 and 11). The stroma associated with the ventral portion of the PUG and PUC is loose preputial mesenchyme and is located external to the preputial lamina (Figs. 10 and 11). The preputial lamina defines the future penile surface, and penile stroma is situated internal (deep) to the preputial lamina.

The separation of the urethra from the PUC within the distal portion of the developing penis involves an epithelial fusion event indicated in Fig. 10F (large black arrow) and Fig. 11E. The epithelial fusion results in a transitory epithelial seam (Fig. 10E), which more proximally disappears resulting in midline mesenchymal confluence within the prepuce and a stand-alone urethral tube completely surrounded by penile mesenchyme and no longer attached to the preputial lamina (Figs. 10G and 11E-I). These developmental fusion events occur from 16 days of gestation to birth to form the distal portion of the penile urethra, keeping in mind that the proximal portion of the penile urethra forms by direct canalization of the urethral plate.

3.2. Immunohistochemical signatures during mouse penile development

Given the strikingly different histologic signatures of the definitive urethral plate of 14- and 15-day mouse embryos versus that of the occluded VPG, the PUG and the PUC seen at day 16 and thereafter, we examined the immunohistochemical signatures of the these structures as well as that of the urethra and the preputial epidermis. For this purpose immunohistochemical assays were performed for the following proteins: androgen receptor (AR), Foxa1, keratins 6, 7, 8, 10, 14 and 19

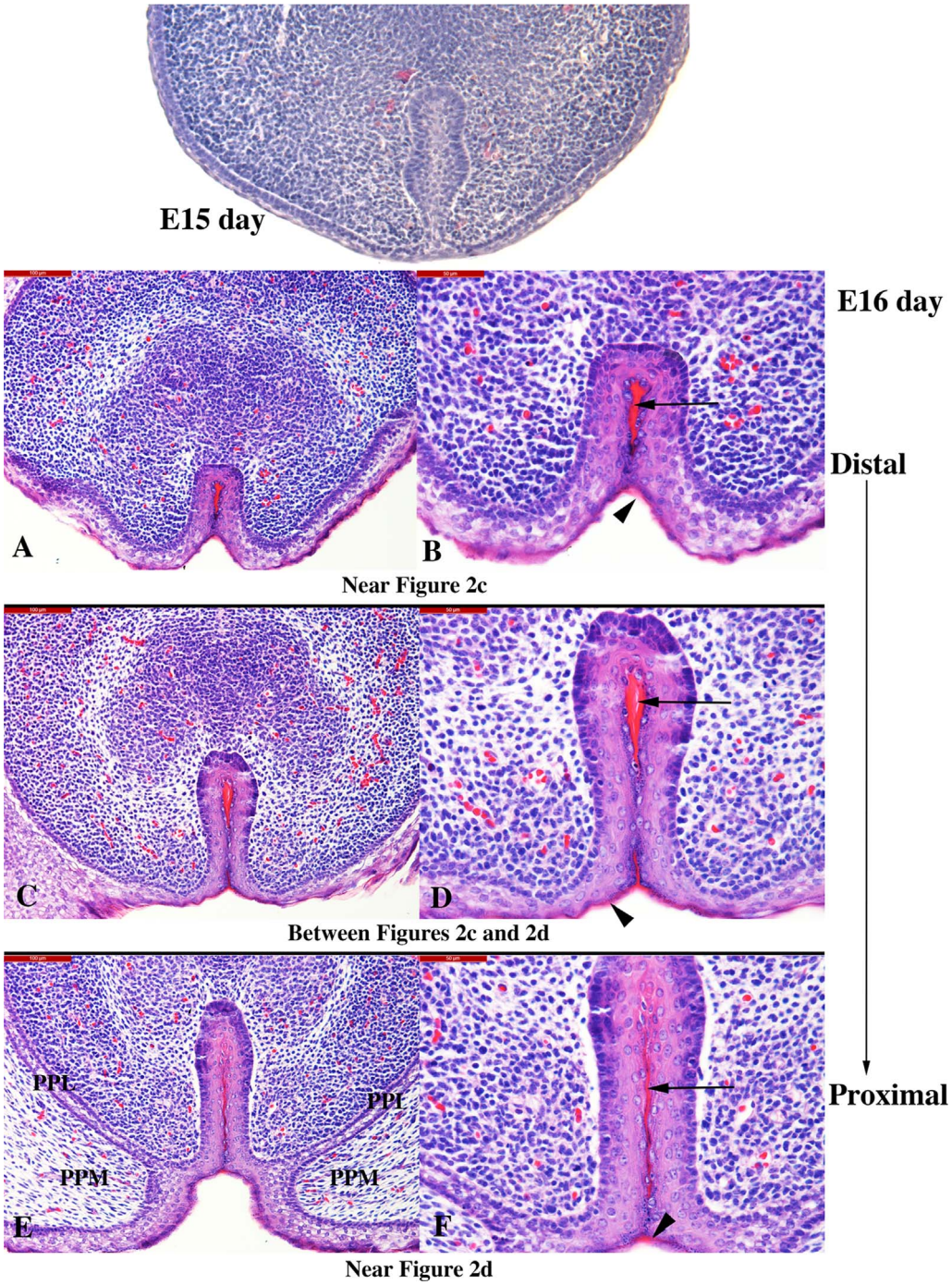

Fig. 7. The histologic profiles of the E15-day urethral plate (top) and the E16-day occluded ventral penile groove at distal (A & B), intermediate (C & D) and proximal (E & F) positions (low and high magnification). Note the eosinophilic stratum corneum of the epidermis and the accumulation of similar eosinophilic non-nucleated squames trapped within the occluded ventral penile groove (arrows) and the complete absence of these features in the E15-day urethral plate.

and uroplakin on external genitalia of 14, 16, 17 and 18 mice (Fig. 12). These data represent a comprehensive immunohistochemical survey of the embryonic urethral plate, the ventral penile groove, the PUG, the PUC, the urethra and the preputial epidermis, which allows insight into the developmental relationships between these structure and perhaps germ layer of origin. The 4 most informative markers are the androgen receptor (AR), Foxal, keratin 7 and keratin 10. These markers are highlighted in color to draw attention to important differences in marker expression in these structures.

Foxa1 is a known endodermal marker (Diez-Roux et al., 2011; Robboy et al., 2017; Besnard et al., 2004) and is normally expressed in epithelium of the developing and adult bladder, urethra and gastro-intestinal system (Kwon et al., 2006; Sun et al., 1999; Robboy et al., 2017). Foxa1 was expressed (a) in the 14 and 15 day urethral plate, (b) in the “stand-alone” urethra at all ages, but (c) was not detected in preputial epidermis (Figs. 12 and 13B & D). These observations are consistent with endodermal derivation of the urethral plate and ectodermal derivation of epidermis as suggested previously (Seifert

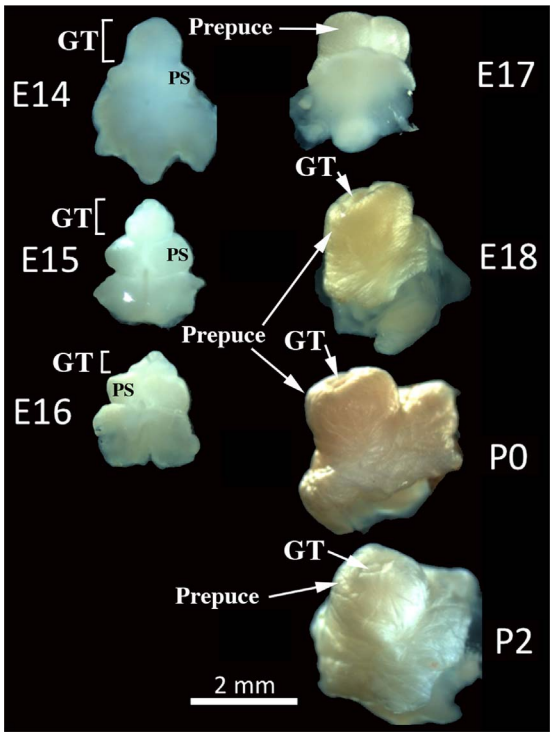

Fig. 8. Wholemount images of mouse GTs at E14 to P0 as ventral views. The preputial swellings (PS) enlarge and fuse in the midline to form the prepuce, which extends distally to eventually completely cover the genital tubercle (GT) at E18, P0 and P2).

et al., 2008). The remaining protein markers cannot be interpreted relative to germ layer origin, but reinforce gene expression differences between these structures.

We have identified two epithelial plates in the course of this study, the definitive urethral plate seen at E14 and E15 and the occluded ventral penile groove seen at E16. As stated above these two structures have different histological signatures. The 14-day (and 15-day, not illustrated) solid urethral plate expresses AR and Foxa1, but not K10, a pattern identical to that of the urethra (Fig. 13A & B). In contrast, the 16-day occluded ventral penile groove lacks AR, strongly expresses K10, and Foxa1 is expressed in only a minor subset of cells dorsally (Fig. 14). This Foxa1 expression in the occluded ventral penile groove (distal to the urethral plate) may be indicative of endodermal cells that have migrated distally from the urethral plate. This pattern of expression of AR and K10 in epithelial cells of the occluded ventral penile groove precisely resembles that of skin with which it is in continuity (Fig. 14). The important point is that the immunohistochemical profile of the definitive urethral plate seen at E14 and E15 is substantially different from that of the occluded ventral penile groove even though both exhibit plate-like morphology. Many differences exist between the urethral plate and the occluded ventral penile groove: (a) From analysis of serial histologic and serial OPT sections, it is evident that the occluded VPG develops distal to the urethral plate as described above. (b) Development of these structures occurs on a different temporal schedule. The urethral plate can be recognized from E12 to E15 (Hynes and Fraher, 2004a) and at E16 is canalized to its distal extremity (Figs. 1, 2, 4), while the occluded VPG is seen on day E16 only (Fig. 7). (c) The urethral plate and the occluded ventral penile groove have vastly different histologic and immunohistochemical profiles. (d) The histologic and immunohistochemical profiles of the occluded VPG are almost identical to that of epidermis, consistent with the idea that the occluded VPG is an ectodermal derivative while the urethral plate is an endodermal derivative based upon Foxa1 staining and LacZ staining reported previously (Seifert et al., 2008). The single exception to this idea is the presence of a subset of Foxa1 cells in the dorsal portion of the occluded VPG, suggesting partial contribution of endodermal cells (presumably derived for the urethral plate) to the occluded VPG, which will be discussed in greater detail below.

From E16 to E18 the PUG forms as the preputial swellings approach the ventral midline, the PUC forms as the edges of the PUG fuse, and ultimately the penile urethra develops as a dorsal subdivision of the PUC (Figs. 10–11). We believe that the PUG and PUC represent the developmental interface between endoderm and

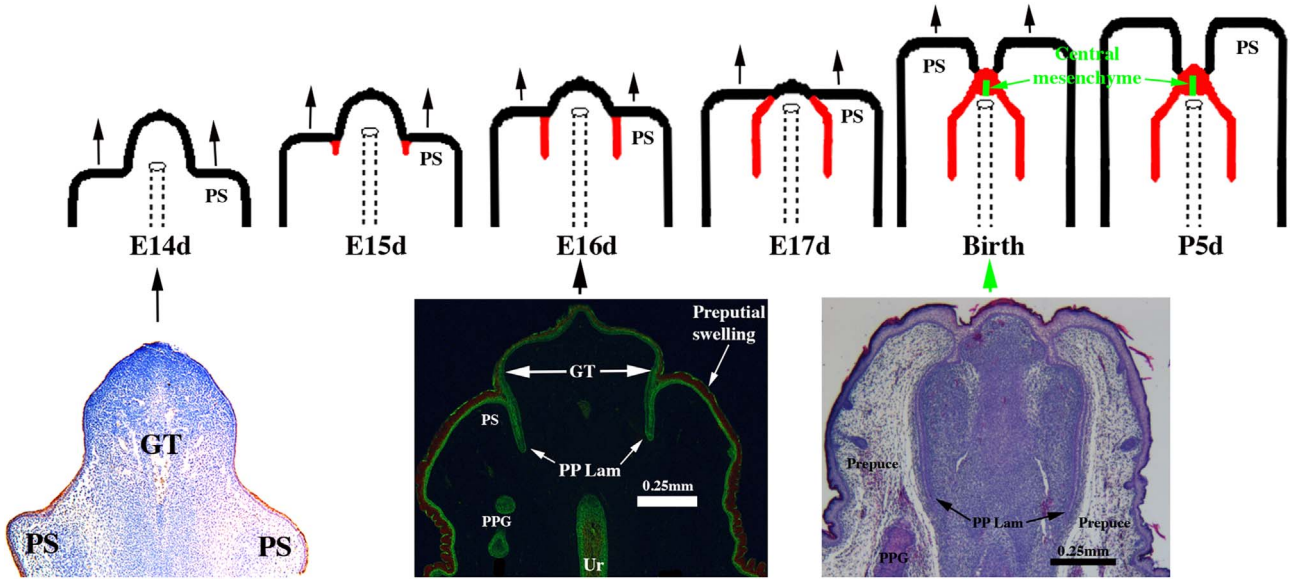

Fig. 9. Diagrammatic representations of development of the prepuce and the preputial lamina (red) from the preputial swellings (PS). Coronal histologic sections depict the process at E14, E16 and P0. In the diagram note that as the prepuce grows distally the preputial lamina (red) is "left in its wake" and thus with time the length of the preputial lamina increases. Black arrows indicate distal growth of the prepuce. The dotted lines represent the urethra. At birth a complex central epithelium forms into which grows a central core of mesenchyme (green), which is the precursor of the male urogenital mating protuberance (MUMP, see Fig. 17). GT=genital tubercle, PPG=preputial gland, PP Lam=preputial lamina, PS=preputial swelling. (For interpretation of the references to color in this figure legend, the reader is referred to the web version of this article.)

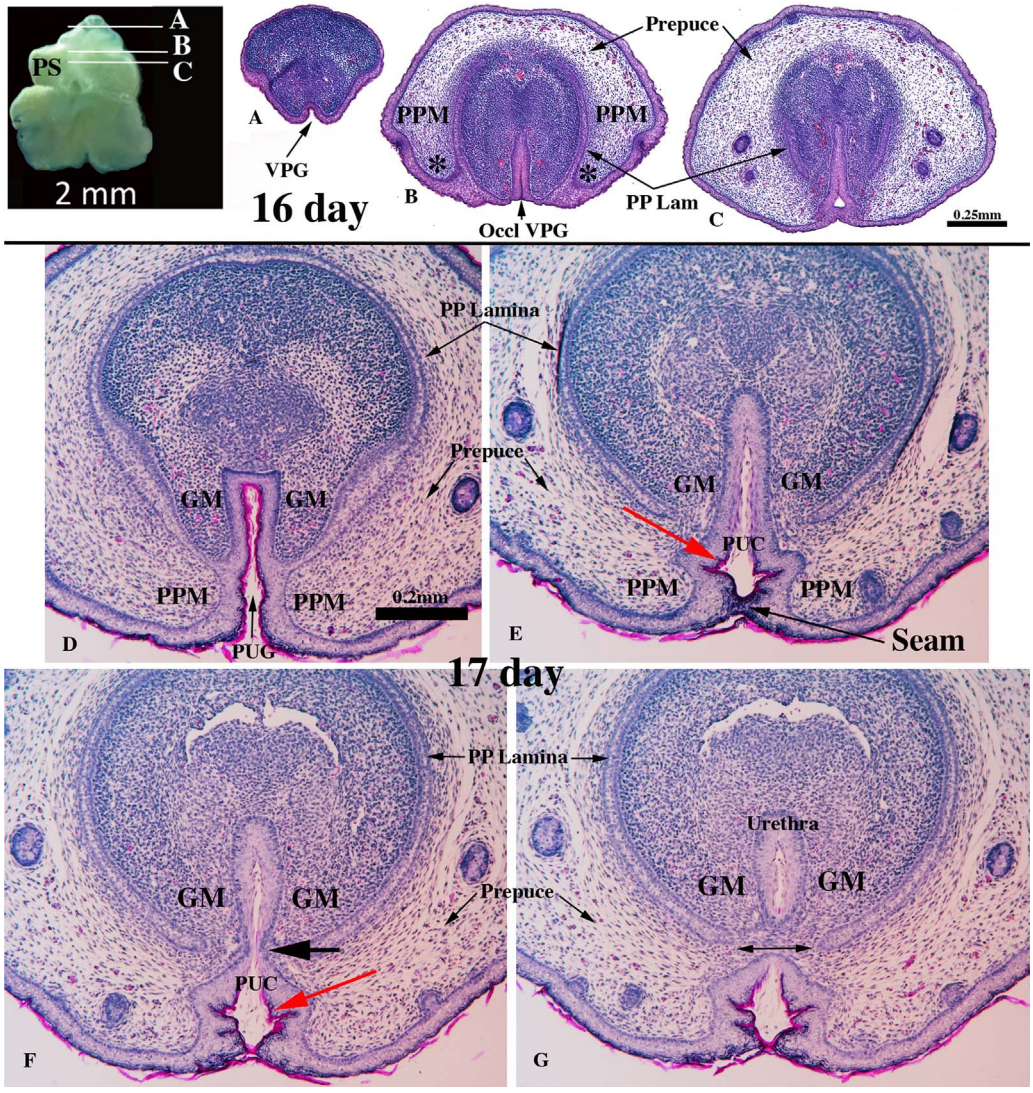

Fig. 10. 16-day wholemount and sections of E16 and E17 external genitalia. Sections A-C are taken at the levels indicated in the wholemount. Section (A) is a distal section at the level of the shallow ventral penile groove (VPG). Section (B) is more proximal at the level of the occluded ventral penile groove (Occl-VPG). Asterisks in (B) depict the preputial swellings growing towards the ventral midline. Section (C) is even more proximal showing canalization of the occluded ventral groove. Sections (D-G) are from 17-day external genitalia showing in (D) the preputial-urethral groove (PUG), in (E) the preputial-urethral canal (PUC), in (F) the point of secondary fusion (large black arrow) within the PUC to segregate the urethra, and in (G) the "stand alone" urethra within the dense mesenchyme of the glans (GM) surrounded by the preputial lamina. Double-headed arrow in (G) indicates midline mesenchymal confluence. The large red arrows in (E & F) draw attention to the eosinophilic stratum corneum in the ventral portion of the PUC. PP Lamina= preputial lamina, PPM=preputial mesenchyme, GM= penile glans mesenchyme. (For interpretation of the references to color in this figure legend, the reader is referred to the web version of this article.)

ectoderm, and accordingly these structures exhibit histologic and immunohistochemical profiles intermediate between that of the endodermal urethral plate and epidermis. The markers of the urethral plate consist of the following: AR, Foxa1 (Fig. 13) and K7 (Fig. 12). The PUG and PUC also express AR, K7 and Foxa1 (but only dorsally), but in addition the PUG and PUC express K10 (Fig. 12). Close examination of the PUC (Fig. 10E & F) reveals an interesting dorsal-ventral difference in histology. The dorsal portion of the PUC is devoid of cornified squames, while the ventral portion of the PUC has a definite stratum corneum (Fig. 10E & F, red arrows). Associated with this distinct dorsal-ventral histologic difference is the dorsal expression of Foxa1 in the PUG and PUC. Indeed the extent of Foxa1 expression increases from distal to proximal in the PUG and PUC (Fig. 15).

Once a fully formed urethra has developed from the dorsal portion of the PUC, the urethral epithelium expresses AR, keratins 7 and 10, Foxa1 and uroplakin (Fig. 16). Thus, K10 expression is shared by epithelium of the urethra and the epidermis, while the AR, Foxa1 and K7 are only expressed in urethral epithelium and not in epidermis.

In summary, from 16 days to birth the distal portion of the penile urethra develops from the PUG and PUC during a process whereby the prepuce grows distally to completely cover the GT. At 16 days of gestation the shallow ventral penile groove expands dorsally as the occluded ventral penile groove, which subsequently canalizes. As the preputial folds approach the midline the PUG is defined. The edges of the PUG fuse in the ventral midline to form the preputial-urethral canal (PUC), which is associated with both preputial mesenchyme as well as penile stroma. Subsequently, the PUC is subdivided by a secondary fusion event into the penile urethra dorsally and a residual canal/groove that eventually will disappear.

A critically important issue regarding the development of the distal portion of the mouse urethra is "where precisely is it taking place relative to the distal portion of the urethral plate"? At 16 days of

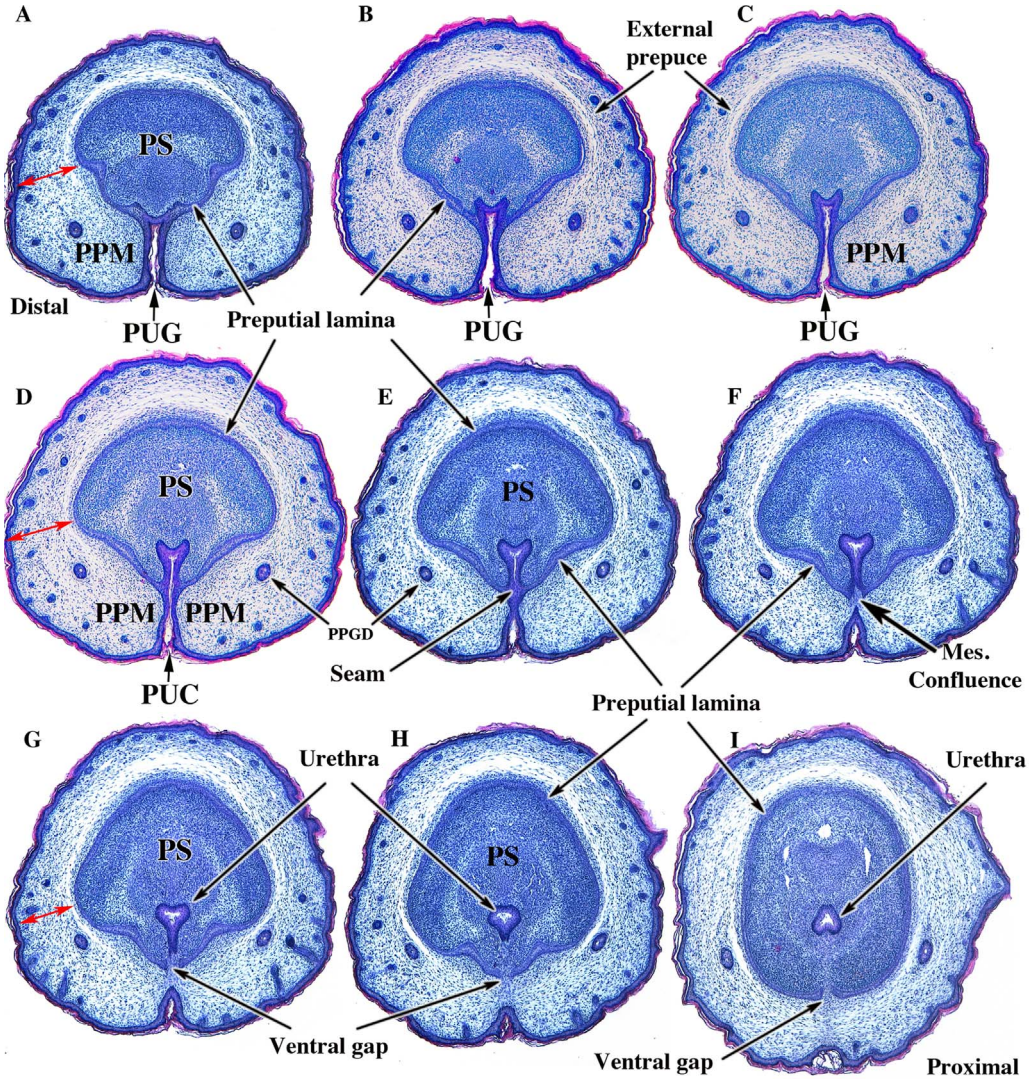

Fig. 11. Transverse sections of the external genitalia of a newborn male CD-1 mouse. Sections are arranged from distal (A) to proximal (I). In (A) the right and left preputial swelling are approaching the ventral midline forming the preputial-urethral groove (PUG), also seen in (B & C). The prepuce (double-headed red arrows in A, D & G) has a thick wall of loose mesenchyme (PPM). The penis is surrounded by the preputial lamina (A-I) and consists of dense penile stroma (PS). In (D & F) the PUG is fusing ventrally to complete the prepuce and form the preputial-urethral canal (PUC). In (E) a secondary fusion has formed a transitory seam, which disappears in (F & G) to segregate the urethra and establish midline mesenchymal confluence. Connections between the urethral epithelium and the preputial lamina (E & F) also are eliminated in more proximal sections resulting in a "stand alone" urethra (G-I). Adapted from Sinclair (2016a) with permission.

gestation the canalized urethral plate terminates distally about 1 mm from the tip of the GT (Figs. 1–3). The fundamental question is what develops from that portion of the GT distal to the "urethral meatus" at 16 days of gestation. Additionally, how does the developmental fate of the distal portion of the GT relate to adult penile morphology? Two possibilities emerge. (1) The urethral meatus seen at E16 days may become the definitive adult urethral meatus, and accordingly the portion of the GT distal to the 16 day meatus may become the adult MUMP (see Fig. 17). (2) An alternate possibility is that the urethra continues to develop distally through formation of the PUG and fusion of its edges to form the PUC from which forms the distal portion of urethra. Our data support this later possibility since the distal growth and ventral fusion of the preputial swellings completely covers and grows distal to the tip of the GT (Figs. 8 and 9). Eventually the prepuce extends distally well beyond the developing GT. In the course of preputial development the PUG and PUC form largely from preputial tissues that ultimately give rise to the distal portion of the penile urethra (Figs. 10 and 11). Note at 16 days that the urethral meatus (the distal terminus of the canalized urethral plate) is at the proximal-distal position of the preputial swellings (Figs. 1–2), while at later stages the preputial swellings grow distally to completely envelope the GT (Figs. 8 and 9) to form the PUG and subsequently the PUC (Figs. 10–11), thus extending the urethra distally.

Finally, there is the question of how does the development of the MUMP (Fig. 17) relate temporally and spatially with the development of the distal portion of the penile urethra? From a detailed morphometric analysis (Schlomer et al., 2013), the distally bifid MUMP appears shortly after birth from "central mesenchyme" circumscribed by epithelium (Fig. 9) and the bilateral "dorsal mesenchymal columns" that appear on days 2–3 postnatal and extend distally from the "central mesenchyme" to form the bifid tip of the MUMP (Schlomer et al., 2013). These data, taken together, support the idea that the distal portion of the penile urethra of the mouse seen at 16 days of gestation extends distally as a result of growth of the preputial swellings to form

14 day

	Distal plate	Proximal plate	Canalized plate	Urethra	Epidermis
AR	-/+	-/+	+	+	-
Foxa1	+	+	+	+	-
K6	+	+	+	+	+
K7	-	+	+	+	-
K8	-	-	-	-	-
K10	-	-	-	-*	-/+
K14	+	+	+	+	+
K19	-	-	-	-	-
Uroplakin	-	-	-	-	-

16 day

	Occluded VPG	PUG	Urethra	Epidermis
AR	-	+	+	-
Foxa1	Dorsal +	Dorsal +	+	-
K6	+	+	+	+
K7	-	+	+	-*
K8	-	+	-	-
K10	+	+	+	+
K14	+	+	+	+
K19	-	-	+	-
Uroplakin	-	-	+	-

17 day

	PUG	PUC	Urethra	Epidermis
AR	+	+	+	-
Foxa1	Dorsal +	Dorsal +	+	-
K6	+	+	+	+
K7	+	+	+	-*
K8	+	+	-	-
K10	+	+	+	+
K14	+	+	+	+
K19	-	+	+	-
Uroplakin	-	-	+	-

18 day

	PUG	PUC	Urethra	Epidermis
AR	+	+	+	-
Foxa1	Dorsal +	Dorsal & Ventral +	+	-
K6	+	+	+	+
K7	+	+	+	-*
K8	+	+	-	-
K10	+	+	+	+
K14	+	+	+	+
K19	-	-	+	-
Uroplakin	-	-	+	-

Fig. 12. Charts summarizing the immunohistochemical profiles of developing mouse external genitalia at 14, 16, 17 and 18 days of gestation. AR=androgen receptor, K6- K19 = keratins 6–19. The colored entries are those that either change with time or depict important differences in expression between the various structures.

the PUG and the PUC, whose development is intimately related to development of the prepuce. A subsequent epithelial fusion event within the PUC (Figs. 10–11) segregates the urethra from the ventral portion of the PUC thus forming the distal portion of the mouse penile urethra and completing development of the prepuce via ventral midline fusion of the preputial swellings.

Another important question is the germ layer origin of the epithelium of the distal portion of the mouse penile urethra, specifically the region of epithelial fusion events as described above. Based upon LacZ staining of the Shh-GFPcre;R26R mice as well as a Msc2cre;R26R mice, it has been proposed that "the (mouse) glandar urethra is derived entirely from endoderm and the ectoderm makes no detectable contribution" (Seifert et al., 2008). Both Shh and Osr1 promoters have been used previously to identify the endodermal lineage, even though both transgenic mice show LacZ staining in non-endodermal cells (Seifert et al., 2008; Grieshammer et al., 2008). Curiously, with regard to the embryonic urethral plate the LacZ staining pattern differs in the Seifert and Grieshammer studies. Seifert using "Shh-LacZ mice" shows LacZ staining throughout the urethral plate (Seifert et al., 2008). Grieshammer using "Osr1-LacZ mice" show LacZ staining only in the dorsal portion of the urethral plate at a comparable age (Grieshammer et al., 2008). These two disparate observations have important developmental implications in regard to the germ layer origin of the urethral plate, and the distal portion of the urethra. Our histologic and immunohistochemical observations provide insight into this question. It is striking that the epithelium of the ventral penile groove and the preputial-urethral groove are continuous laterally with penile or preputial epidermis and exhibit a histologic and immunohistochemical signature remarkably similar to that of epidermis, which is certainly ectodermal in origin (Figs. 10, 11, 12 and 14). Most important, the PUG is mostly devoid Foxa1 (an endoderm marker), later only expressing it in an extremely restricted fashion (Fig. 15A).

Seifert et al. used Msx2cre;R26R mice to interrogate the possible ectodermal contribution to the glandar urethra and interpret their findings as indicating that the mouse "glandar urethra is derived entirely from endoderm and that ectoderm makes no detectable contribution" (Seifert et al., 2008). The justification of using Msx2cre;R26R mice for the purpose of investigating ectodermal lineage was that the authors had "found previously that Msx2 is expressed in the ectoderm overlying the developing genital tubercle at E11.5" (Seifert et al., 2008). Further validation of this approach through analysis of Msx2-LacZ staining throughout the embryo, especially in cornified versus non-cornified ectodermal cells was not presented. Careful examination of Fig. 4C in Seifert et al. shows LacZ staining in the apical-most layer (stratum corneum) of penile epidermis and a complete absence of LacZ staining in the urethra. None of the other epidermal layers (stratum basale, stratum spinosum, stratum granulosum, stratum lucidum) were LacZ stained. This curious finding raises the possibility the LacZ staining seen in "Msx2-LacZ mice" reflects terminal epidermal differentiation in the stratum corneum. Thus, Msx2-LacZ staining may be questionable as a marker of ectodermal germ layer origin, and in any case "Msx2-LacZ mice" have not been properly validated in regard to ectodermal lineage. It is important to note that ectoderm gives rise to both fully cornified epithelia, as is the case for epidermis, as well as non-cornified epithelia, as is the case for cornea and oral epithelia. Do Msx2-LacZ mice exhibit LacZ staining in

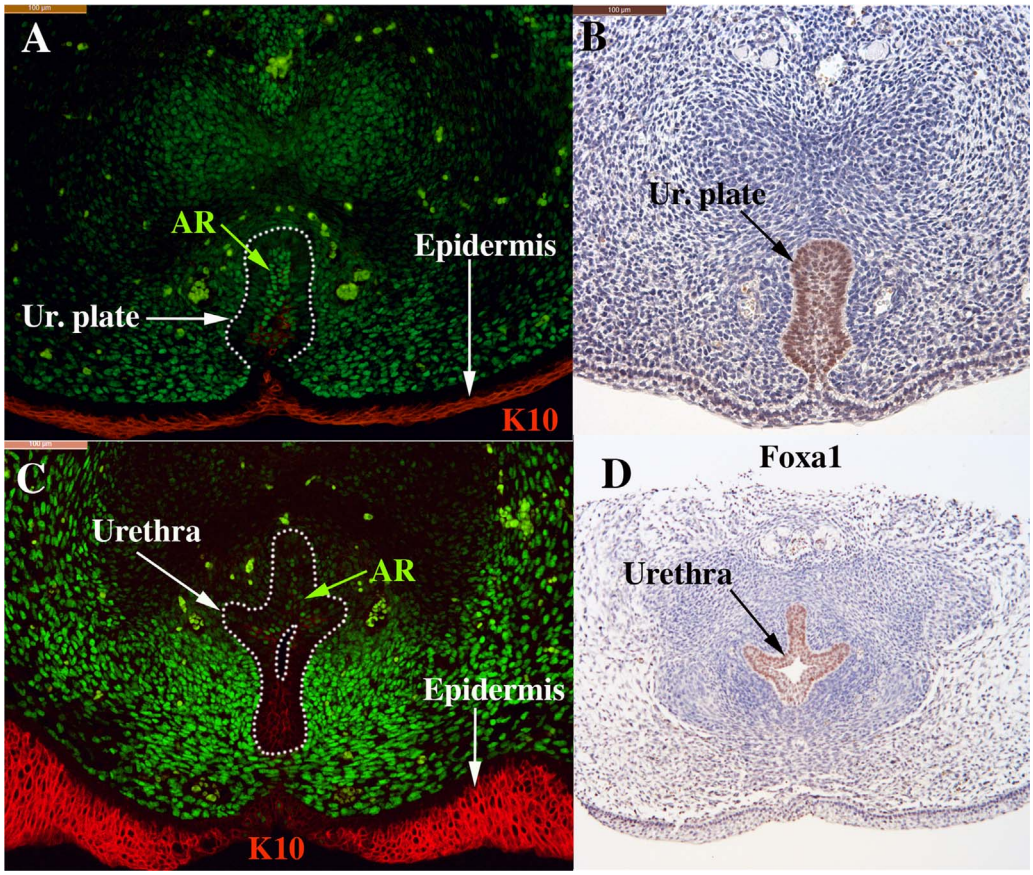

Fig. 13. Immunohistochemical profiles of the solid urethral plate (Ur. Plate) attached to the epidermis (A & B) and the urethra (canalized urethral plate) (B & D). (A & C) depict androgen receptor (AR) in green and keratin 10 (K10) in red. Note the striking difference in AR and keratin 10 in the epidermis versus the urethral plate and urethra. (B & D depict Foxal expression in the urethral plate (B) and the urethra, but not in the epidermis. All sections are from an E14 mouse embryo. (For interpretation of the references to color in this figure legend, the reader is referred to the web version of this article.)

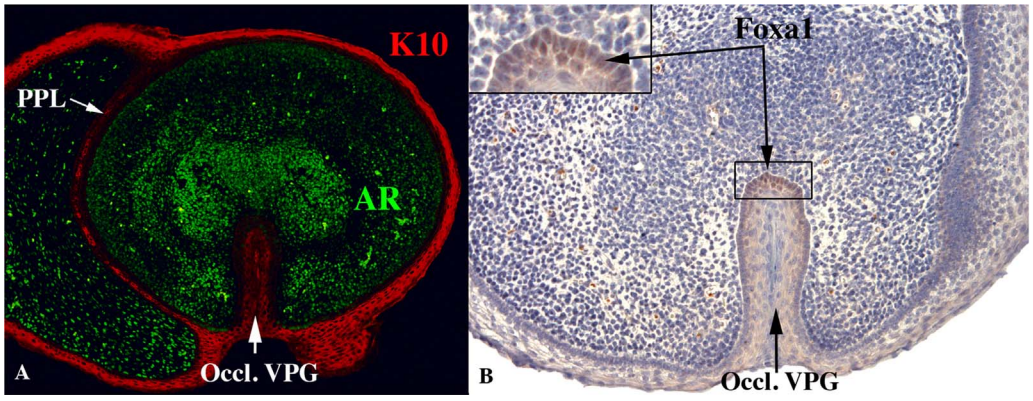

Fig. 14. Sections of E16 GTs stained for keratin 10 (red) and androgen receptor (A, green) and Foxa1 (B). The occluded ventral penile groove expresses keratin 10 (K10) and Foxa1 in a small subset of dorsally located epithelial cells (B and inset), but not androgen receptor (AR). The epidermis and the preputial lamina (PPL) express keratin 10 and not androgen receptor or Foxa1. (For interpretation of the references to color in this figure legend, the reader is referred to the web version of this article.)

corneal and oral epithelia? Regarding the potential contribution of ectoderm to the mouse glandar urethra, we concur with Seifert's statement that “these experiments could not exclude the possibility that some ectodermal cells are incorporated into the distal region (of the urethra)” (Seifert et al., 2008). Indeed, the histologic and immunohistochemical profile of the PUG and PUC (from which the distal urethral develops) is consistent with ectodermal derivation. In any case, the relation of germ layer lineage studies performed during development to the adult penile urethra remains to be deterimined.

The idea that the distal portion of the mouse penile urethra forms as a result of epithelial fusion events is supported by several inferences from adult morphology. The urethral meatus of the adult mouse penis is formed by the male urogenital mating protuberance (MUMP) dorsally and the MUMP ridge ventral-laterally (Rodriguez et al., 2011). The MUMP ridge has a prominent ventral cleft (Figs. 17–18). Our interpretation is that the ventral-lateral portion of the urethral meatus formed via incomplete midline fusion of bilateral elements of the MUMP ridge leaving a prominent ventral cleft. Close examination

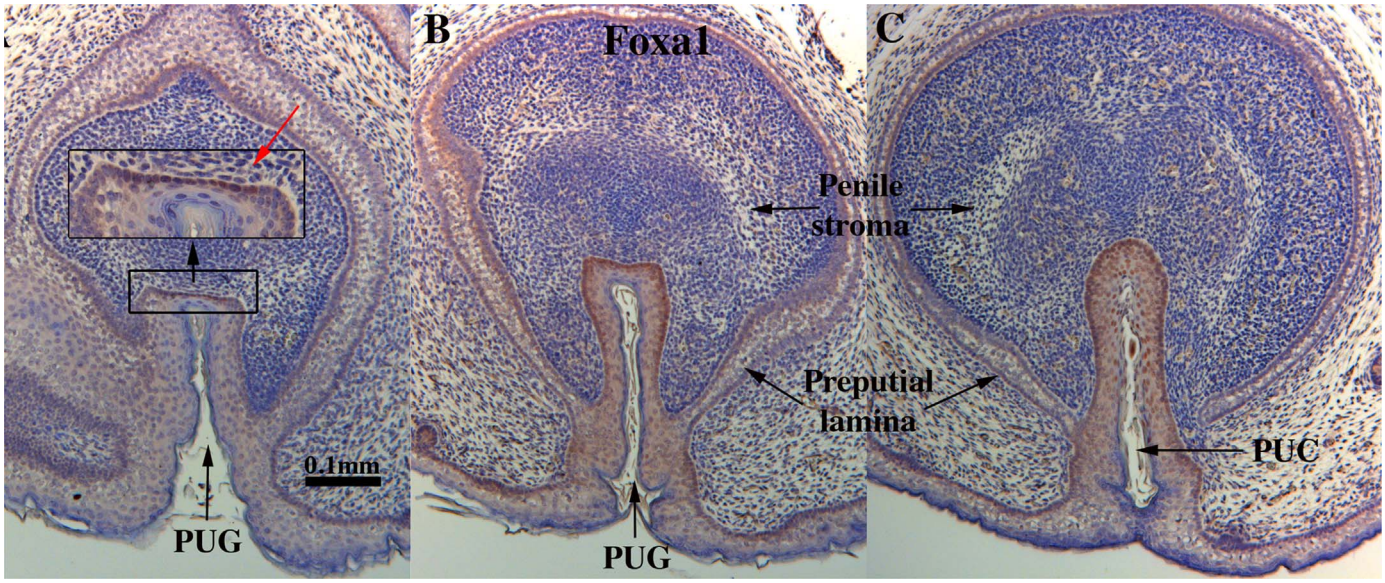

Fig. 15. Sections of the preputial-urethral groove (PUG) and preputial-urethral canal (PUC) at E16 immunostained for Foxa1. The sections are displayed from left to right in distal to proximal order. Distally (A) Foxa1 is expressed in a small subset of dorsally located epithelial cells of the PUG. Progressing proximally (B-C) note the increases in Foxa1-positive epithelial cells in the PUG (B) and in the PUC (C).

of the adult mouse urethral meatus by scanning electron microscopy shows that the dorsally situated MUMP is separated from the MUMP ridge by bilateral clefts/grooves, and the MUMP ridge itself is comprised of bilateral elements separated by clefts/grooves (Fig. 18A-B) (Blaschko et al., 2013). These bilateral clefts/grooves between the MUMP and MUMP ridge and within the MUMP ridge suggest that the urethral meatus formed via multiple fusion events between the MUMP and MUMP ridge and within elements of the MUMP ridge itself. The regular pattern of elements and grooves comprising the adult urethral meatus is perturbed by perinatal diethylstilbestrol (DES) treatment or physiologic elevation of estradiol levels in AROM+ mice, which in both cases elicits profound malformations of the mouse urethral meatus (Blaschko et al., 2013; Sinclair et al., 2016b; Mahawong et al., 2014a, 2014b) (Fig. 18C-D) and is consistent with the idea that elevated estrogen levels perturbed the orderly fusion of the developmental elements constituting the urethral meatus, that is, fusion between the MUMP and MUMP ridge and between the elements that form the MUMP ridge.

Another example of a possible fusion event involves the mouse prepuce. Mice have two prepuces (Blaschko et al., 2013). The external prepuce forms the prominent perineal elevation and creates the preputial space housing the penis, while the internal prepuce is a flap of “skin” this is integral to the penis (Blaschko et al., 2013). The internal prepuce of the mouse also has a ventral cleft (Fig. 17). The inference of this observation is that the internal prepuce also forms by incomplete mid-ventral fusion of bilateral elements. It is perhaps worth noting that the external prepuce is completed ventrally via fusion of the bilateral preputial swellings (Petiot et al., 2005; Perriton et al., 2002; Sinclair et al., 2016a) (Fig. 11). The orderly mid-ventral fusion of the preputial swellings is also profoundly disturbed by perinatal exposure to DES (Mahawong et al., 2014a, 2014b). Thus, fusion events in development of the mouse male external genitalia receive considerable support.

3.3. Development of the human penile urethra

Within the human penile shaft, the urethra develops via formation of the urethral plate, which canalizes to form an open urethral groove whose edges (urethra folds) fuse in the midline to form the tubular urethra (Fig. 19) (Li et al., 2015; Shen et al., 2016). Scanning electron microscopy demonstrated that the urethral groove does not extend into the glans penis suggesting that the urethra within the glans forms via a different morphogenetic mechanism. Serial H & E stained sections and OPT sections (Li et al., 2015) verify the absence of a urethral groove within the glans, and also demonstrate extension of the urethral plate into the glans almost to its distal tip (Fig. 19A). The urethral plate within the glans (Fig. 20A) canalizes directly to extend the penile urethra into the glans (Fig. 20B-E). The process of canalization is asymmetric and begins within the ventral portion of the urethral plate, but progressively expands dorsally (Fig. 20B-E). Additional details of development of the human glandar urethra can be found in a separate publication in preparataion. With respect to canalization of the urethral plate within the human glans, it is important to recognize that the canalization process occurs initially within the ventral portion of the urethral plate, but subsequently extends dorsally within the urethral plate (Fig. 20). Thus, a consistent dorsal-ventral asymmetry is observed within the urethral plate of the glans, which presumably is based upon dorsal-ventral differences in gene expression.

Thus, entirely different morphogenetic mechanisms of penile urethral development occur within the human penile shaft versus the glans. Similarly in the mouse, morphogenesis of the penile urethra is substantially different proximally versus distally near the urethral meatus. In both species, direct canalization of the urethral plate has been revealed, but in the case of humans this occurs distally within the glans, whereas in mice canalization of the urethral plate occurs within the proximal portion of the penis. Fusions events are also common to both mice and humans. In mice, fusion events account for the development of the distal portion of the penile urethra, whereas in humans fusion events are involved in formation of the urethral within the penile shaft.

The idea that the distal portion of the mouse penile urethra, and especially the urethral meatus, forms via requisite fusion events is based upon both inference from adult morphology and direct observations of development. Inferences, based upon adult anatomy of the urethral meatus, are clearly central to our interpretation. In adulthood a ventral cleft partially bisects the MUMP ridge (which forms most of the adult urethral meatus). This singular fact leads naturally to the inference that the MUMP ridge develops from bilateral elements that

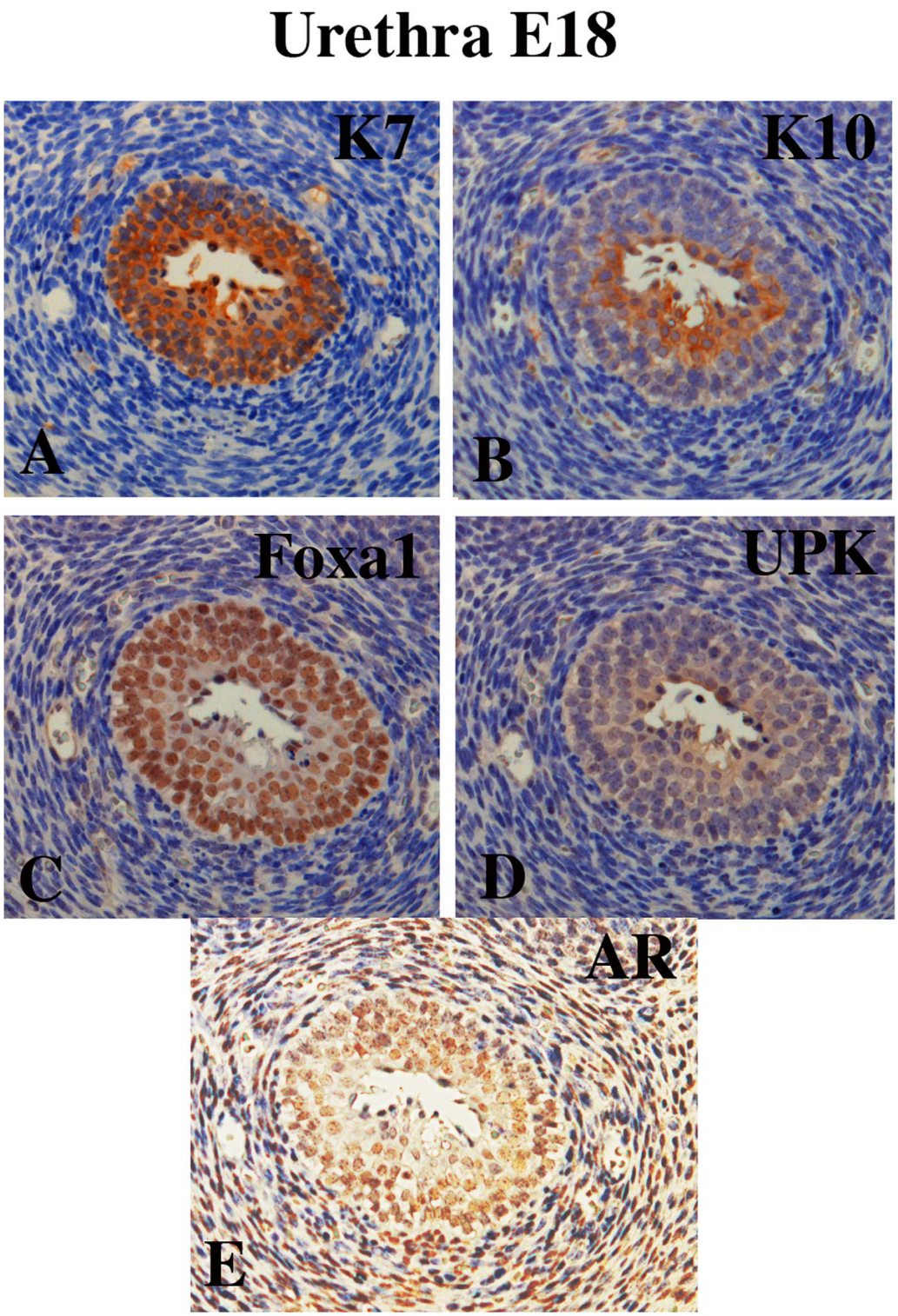

Fig. 16. Section of the E18 penile urethra stained for keratin 7 (K7), keratin 10 (K10), Foxa1, uroplakin, and androgen receptor (AR).

fuse partially resulting in the prominent ventral cleft in the MUMP ridge. This argument is supported by many examples in vertebrate developmental biology, anatomy and congenital malformations observed in humans, mice and wildlife animals. For those structures known to develop via fusion of bilateral elements (tongue, lip, nose, palate, skull, vaginal vestibule, scrotum, anterior body wall, etc.), the fusion process is manifested in adulthood as persistent grooves (philtrum, and linea alba), raphes (scrotal, buccal, lingual, perineal raphes), sutures between skull bones, the symphysis between pubic bones, or clefts (pudendal cleft in humans and palatal cleft in birds). The human pudendal cleft, into which the vagina and urethra open, is defined laterally by the labia majora, derived by the bilateral embryonic labioscrotal swellings that naturally fail to fuse in the midline. In males the labioscrotal swellings fuse in the midline to form the scrotum, and

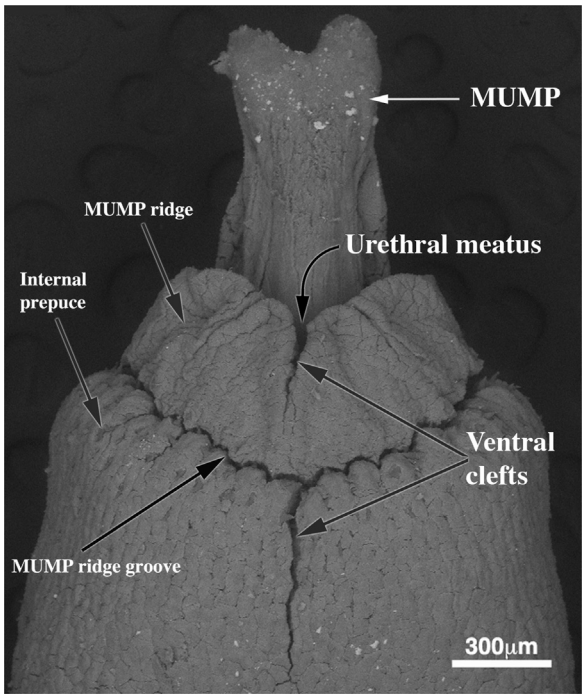

Fig. 17. Scanning electron micrograph of the adult mouse penis (ventral view). Note the MUMP extending distal to the meatus and the ventral clefts in the MUMP ridge and internal prepuce. From Blaschko et al. (2015) with permission.

this fusion event is manifest in adulthood as the scrotal raphe (Clemente, 1985). In the chicken, bilateral palatal shelves form, grow towards the midline and make contact, but fail to fuse resulting in a persistent cleft palate (Shah and Crawford, 1980). Implicit in the wide range of congenital malformations (cleft lip, cleft palate and hypospadias) is the failure of fusion events (midline or lateral). Thus, raphes, grooves, and clefts seen in adulthood are manifestations of developmental fusion events during development. When fusion is incomplete clefts result. Such clefts may be normal (pudendal cleft) or abnormal (cleft lip). Accordingly, the ventral clefts in the adult MUMP ridge and internal prepuce are interpreted as normal incomplete developmental fusion events. The presence of enduring clefts between the MUMP and the MUMP ridge as well as several clefts within the MUMP ridge suggest that the mouse urethral meatus formed via multiple fusions of sub-elements to create the bilateral halves of the MUMP ridge and subsequent fusion of the MUMP with the MUMP ridge. Finally, the profoundly distorted pattern of processes and abnormal clefts seen in the urethral meatus of perinatally DES-treated mice (Mahawong et al., 2014a, 2014b; Blaschko et al., 2013; Cunha et al., 2015) are consistent with the perturbation of fusion events in the development of the urethral meatus of mice.

There is no doubt that urethral plate plays a central role in development of the penile urethra in both mice and humans (Cunha et al., 2015; Armfield et al., 2016). When initially formed at E12 in mice, the urethral plate extends to the distal portion of the genital tubercle (Hynes and Fraher, 2004a). However, at E13 the urethral plate terminates proximal to the distal tip of the GT (Hynes and Fraher, 2004c). Serial histologic sections as well as OPT sections of E14 to E18

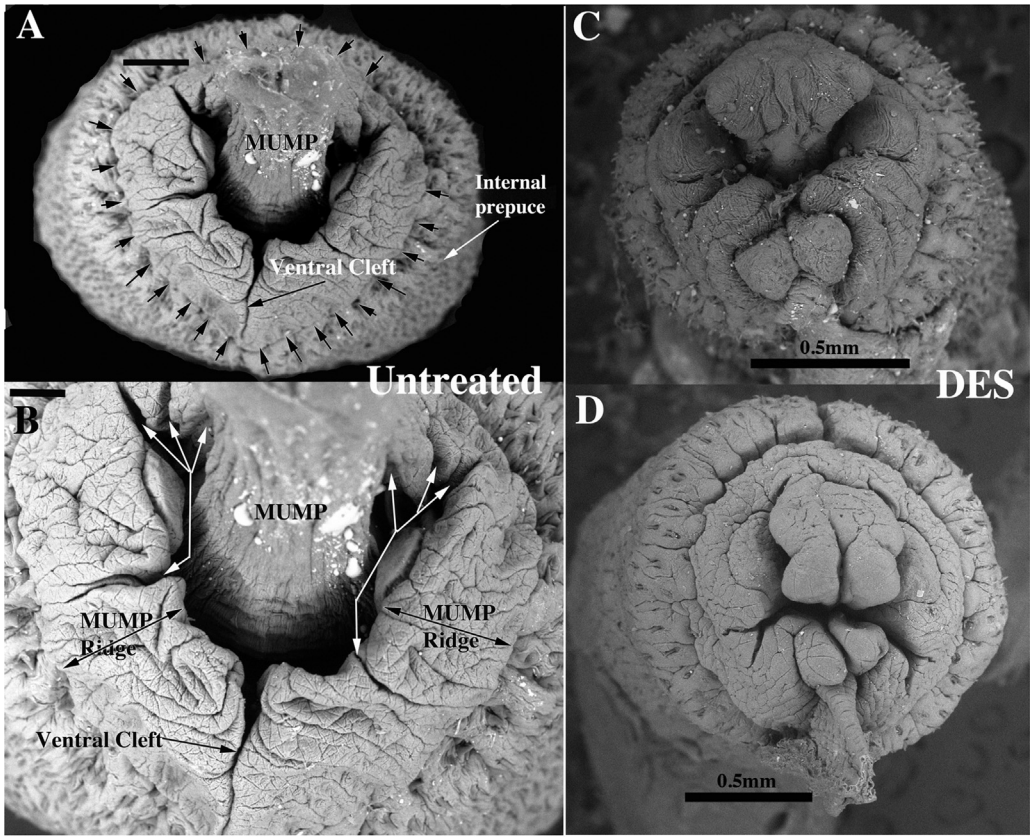

Fig. 18. Scanning electron micrographs of an adult mouse penis, distal end-on views. The urethral meatus is Y-shaped with the ventral cleft in the MUMP ridge being the ventral stem of the "Y". The MUMP, which is projecting towards the viewer, is dorsally situated and is separated from the MUMP ridge by bilateral grooves. The MUMP ridge is demarcated peripherally by the circumferential MUMP ridge groove (small black arrows in [A]). The MUMP Ridge is almost completely bisected by a ventral cleft. The MUMP Ridge has several minor clefts (White arrows in [B]). (C & D) 60-day-old mice treated with DES (200 ng/g of body weight) from birth to day 10. Striking disturbances in the "end-on" morphology are evident that include shortening of the MUMP, abnormal morphology of the MUMP, profound disturbance in the patterning of clefts and processes within the MUMP ridge that include absence of the ventral cleft and the presence of a frenulum-like ventral tether attached to the inner surface of the external prepuce. Thus, the neonatally DES-treated mouse has a grossly abnormal urethral meatus. Scale bars = 200 μm for (A), 100 μm for (B). Modified from Blaschko et al. (2013) and Cunha et al. (2015) with permission.

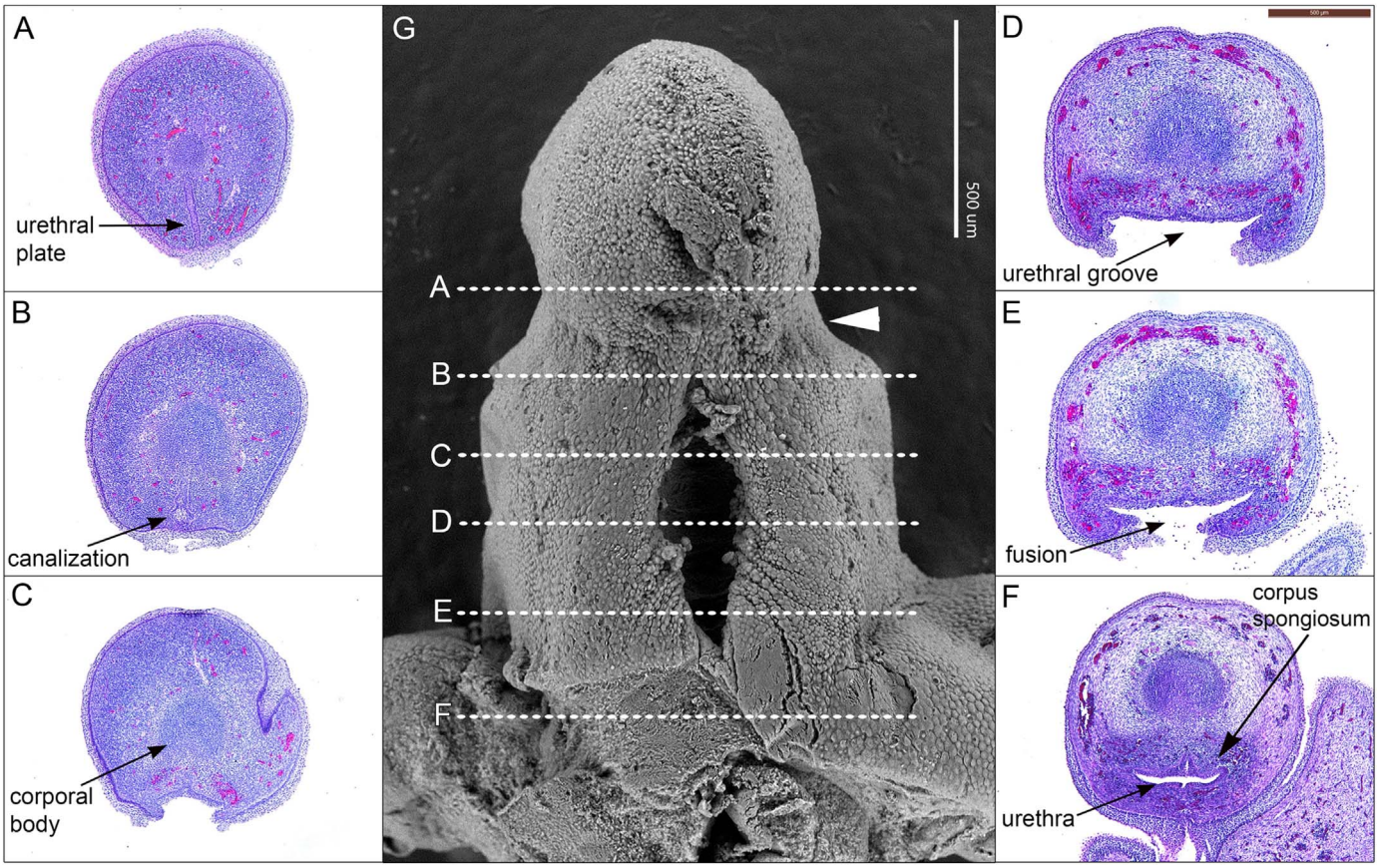

Fig. 19. Scanning electron micrograph (G) and transverse sections of a 9-week human fetal penis stained with hematoxylin and eosin demonstrating (A) the solid urethral plate, (B) the beginning of canalization of the urethral plate, (C) the urethral plate has canalized to from an open urethral groove in the distal penile shaft, (D) mid-shaft showing a widely open urethral groove, (E) beginning of the process of fusion of the urethral folds, and (F) fully formed urethra at the levels indicated in (G). White arrowhead in (G) indicates the transition from penile shaft to glans. Modified from (Shen et al., 2016) with permission.

mouse GTs verify that the urethral plate does not extend to the distal tip of the GT, which calls into question idea that the urethral plate forms the entire penile urethra as suggested (Seifert et al., 2008).

The interface in humans between the disparate mechanisms of penile urethral development (direct urethral plate canalization and urethral fold fusion) occurs at the junction of the glans and the shaft, which is the zone of the highest incidence (50%) of (mild) hypospadias (Carmichael et al., 2005; Baskin, 2017). A mouse anatomical and teratologic counterpart to this human condition has not been reported. Indeed in mice most malformations of the penile urethra are seen exclusively in distal structures that we propose develop via epithelial fusion events (Mahawong et al., 2014a, 2014b; Sinclair et al., 2016b, 2016a; Blaschko et al., 2013; Kim et al., 2004). Genetic manipulations that elicit cloacal anomalies are secondarily associated with severe penile malformations including penile agenesis (Dravis et al., 2004; Yucel et al., 2004). Clearly the mouse is far from perfect as a model for human hypospadias. Urethral development in mice and humans both involve fusion events, but these occur in diametrically different regions, and thus mouse “hypospadias” is an entity substantially different from human hypospadias (Cunha et al., 2015).

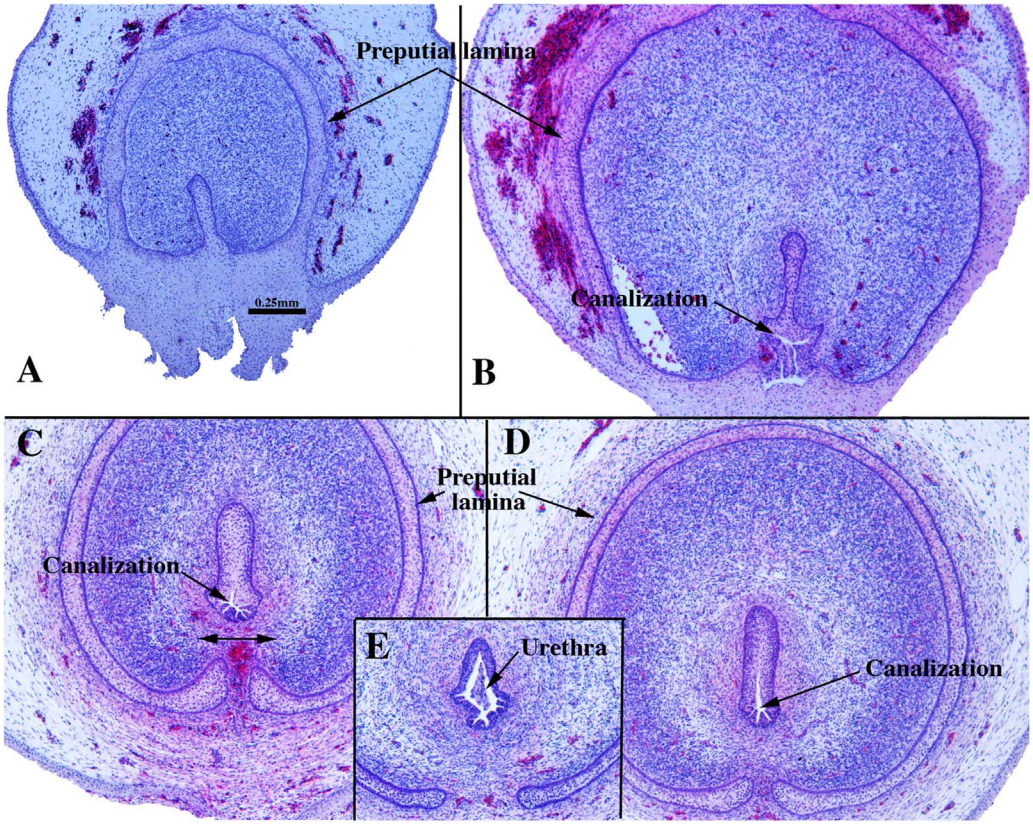

Fig. 20. Sections through the human penile glans at 14 (A, C-E) and 15 weeks (B) of gestation arranged in distal (A) to proximal (E) order. In (A) note the solid urethral plate near the tip of the glans, which is surrounded by the preputial lamina. In (B) the urethral plate is canalizing at its junction with the epidermis. In (C) mesenchymal confluence (double-headed arrow) has been established ventral to the canalizing urethral plate whose dorsum is still solid. In (D) the canalization process is extending dorsally. In (E) a fully canalized urethra has developed.

References

Agras, K., Shiroyanagi, Y., Baskin, L.S., 2007a. Progesterone receptors in the developing genital tubercle: implications for the endocrine disruptor hypothesis as the etiology of hypospadias. J. Urol. 178, 722–727.

Agras, K., Willingham, E., Liu, B., Baskin, L.S., 2006. Ontogeny of androgen receptor and disruption of its mRNA expression by exogenous estrogens during morphogenesis of the genital tubercle. J. Urol. 176, 1883–1888.

Agras, K., Willingham, E., Shiroyanagi, Y., Minasi, P., Baskin, L.S., 2007b. Estrogen receptor-alpha and beta are differentially distributed, expressed and activated in the fetal genital tubercle. J. Urol. 177, 2386–2392.

Armfield, B.A., Seifert, A.W., Zheng, Z., Merton, E.M., Rock, J.R., Lopez, M.C., Baker, H.V., Cohn, M.J., 2016. Molecular characterization of the genital organizer: gene expression profile of the mouse urethral plate epithelium. J. Urol..

Baskin, L., 2017. What is hypospadias? Clin. Pediatr. 56, 409–418.

Baskin, L.S., Erol, A., Jegatheesan, P., Li, Y., Liu, W., Cunha, G.R., 2001. Urethral seam formation and hypospadias. Cell Tissue Res. 305, 379–387.

Baskin, L.S., Liu, W., Bastacky, J., Yucel, S., 2002. Anatomical studies of the mouse genital tubercle. Adv. Exp. Med. Biol. 545, 103–148.

Besnard, V., Wert, S.E., Hull, W.M., Whitsett, J.A., 2004. Immunohistochemical localization of Foxa1 and Foxa2 in mouse embryos and adult tissues. Gene Expr. Patterns: GEP 5, 193–208.

Blaschko, S.D., Mahawong, P., Ferretti, M., Cunha, T.J., Sinclair, A., Wang, H., Schlomer, B.J., Risbridger, G., Baskin, L.S., Cunha, G.R., 2013. Analysis of the effect of estrogen/androgen perturbation on penile development in transgenic and diethylstilbestrol-treated mice. Anat. Rec. 296, 1127–1141.

Butler, C.M., Shaw, G., Renfree, M.B., 1999. Development of the penis and clitoris in the tammar wallaby, Macropus eugenii. Anat. Embryol. 199, 451–457.

Carmichael, S.L., Shaw, G.M., Laurent, C., Croughan, M.S., Olney, R.S., Lammer, E.J., 2005. Maternal progestin intake and risk of hypospadias. Arch. Pediatr. Adolesc. Med. 159, 957–962.

Clemente, C.D. (Ed.), 1985. Gray's Anatomy. Lea and Febiger, Philadelphia.

Cunha, G.R., Risbridger, G., Wang, H., Place, N.J., Grumbach, M., Cunha, T.J., Weldele, M., Conley, A.J., Barcellos, D., Agarwal, S., Bhargava, A., Drea, C., Siiteri, P.K., Coscia, E.M., McPhaul, M.J., Hammond, G.L., Baskin, L.S., Glickman, S.E., 2014. Development of the External Genitalia: perspectives from the Spotted Hyena (Crocuta crocuta). Differ.; Res. Biol. Divers. 87, 4–22.

Cunha, G.R., Sinclair, A., Risbridger, G., Hutson, J., Baskin, L.S., 2015. Current understanding of hypospadias: relevance of animal models. Nat. Rev. Urol. 12, 271–280.

Diez-Roux, G., Banfi, S., Sultan, M., Geffers, L., Anand, S., Rozado, D., Magen, A., Canidio, E., Pagani, M., Peluso, I., Lin-Marq, N., Koch, M., Bilio, M., Cantiello, I., Verde, R., De Masi, C., Bianchi, S.A., Cicchini, J., Perroud, E., Mehmeti, S., Dagand, E., Schrinner, S., Nurnberger, A., Schmidt, K., Metz, K., Zwingmann, C., Brieske, N., Springer, C., Hernandez, A.M., Herzog, S., Grabbe, F., Sieverding, C., Fischer, B., Schrader, K., Brockmeyer, M., Dettmer, S., Helbig, C., Alunni, V., Battaini, M.A., Mura, C., Henrichsen, C.N., Garcia-Lopez, R., Echevarria, D., Puelles, E., Garcia-Calero, E., Kruse, S., Uhr, M., Kauck, C., Feng, G., Milyaev, N., Ong, C.K., Kumar, L., Lam, M., Semple, C.A., Gyenesei, A., Mundlos, S., Radelof, U., Lehrach, H., Sarmientos, P., Reymond, A., Davidson, D.R., Dolle, P., Antonarakis, S.E., Yaspo, M.L., Martinez, S., Baldock, R.A., Eichele, G., Ballabio, A., 2011. A high-resolution anatomical atlas of the transcriptome in the mouse embryo. PLoS Biol. 9, e1000582.

Dravis, C., Yokoyama, N., Chumley, M.J., Cowan, C.A., Silvany, R.E., Shay, J., Baker, L.A., Henkemeyer, M., 2004. Bidirectional signaling mediated by ephrin-B2 and EphB2 controls urorectal development. Dev. Biol. 271, 272–290.

Drey, E.A., Kang, M.S., McFarland, W., Darney, P.D., 2005. Improving the accuracy of fetal foot length to confirm gestational duration. Obstet. Gynecol. 105, 773–778.

Grieshammer, U., Agarwal, P., Martin, G.R., 2008. A Cre transgene active in developing endodermal organs, heart, limb, and extra-ocular muscle. Genesis 46, 69–73.

Hynes, P.J., Fraher, J.P., 2004a. The development of the male genitourinary system: ii. The origin and formation of the urethral plate. Br. J. Plast. Surg. 57, 112–121.

Hynes, P.J., Fraher, J.P., 2004b. The development of the male genitourinary system: III. The formation of the spongiose and glandar urethra. Br. J. Plast. Surg. 57, 203–214.

Hynes, P.J., Fraher, J.P., 2004c. The development of the male genitourinary system. I. The origin of the urorectal septum and the formation of the perineum. Br. J. Plast. Surg. 57, 27–36.

Kim, K.S., Torres, C.R., Jr., Yucel, S., Raimondo, K., Cunha, G.R., Baskin, L.S., 2004. Induction of hypospadias in a murine model by maternal exposure to synthetic estrogens. Environ. Res. 94, 267–275.

Kluth, D., Fiegel, H.C., Geyer, C., Metzger, R., 2011. Embryology of the distal urethra and external genitals. Semin. Pediatr. Surg. 20, 176–187.

Kurzrock, E.A., Jegatheesan, P., Cunha, G.R., Baskin, L.S., 2000. Urethral development in the fetal rabbit and induction of hypospadias: a model for human development. J. Urol. 164, 1786–1792.

Kwon, D.N., Choi, Y.J., Park, J.Y., Cho, S.K., Kim, M.O., Lee, H.T., Kim, J.H., 2006. Cloning and molecular dissection of the 8.8 kb pig uroplakin II promoter using transgenic mice and RT4 cells. J. Cell Biochem. 99, 462–477.

Li, Y., Sinclair, A., Cao, M., Shen, J., Choudhry, S., Botta, S., Cunha, G., Baskin, L., 2015. Canalization of the urethral plate precedes fusion of the urethral folds during male penile urethral development: the double zipper hypothesis. J. Urol. 193, 1353–1359.

Mahawong, P., Sinclair, A., Li, Y., Schlomer, B., Rodriguez, E., Jr., Ferretti, M.M., Liu, B.,

Baskin, L.S., Cunha, G.R., 2014a. Comparative effects of neonatal diethylstilbestrol on external genitalia development in adult males of two mouse strains with differential estrogen sensitivity. Differ.; Res. Biol. Divers. 88, 70–83.
Mahawong, P., Sinclair, A., Li, Y., Schlomer, B., Rodriguez, E., Jr., Ferretti, M.M., Liu, B., Baskin, L.S., Cunha, G.R., 2014b. Prenatal diethylstilbestrol induces malformation of the external genitalia of male and female mice and persistent second-generation developmental abnormalities of the external genitalia in two mouse strains. Differ.; Res. Biol. Divers. 88, 51–69.
Manabe, M., O'Guin, W.M., 1992. Keratohyalin, trichohyalin and keratohyalin-trichohyalin hybrid granules: an overview. J. Dermatol. 19, 749–755.
Mercer, B.M., Sklar, S., Shariatmadar, A., Gillieson, M.S., D'Alton, M.E., 1987. Fetal foot length as a predictor of gestational age. Am. J. Obstet. Gynecol. 156, 350–355.
Mhaskar, R., Agarwal, N., Takkar, D., Buckshee, K., Anandalakshmi, Deorari, A., 1989. Fetal foot length–a new parameter for assessment of gestational age. Int J. Gynaecol. Obstet. 29, 35–38.
Perriton, C.L., Powles, N., Chiang, C., Maconochie, M.K., Cohn, M.J., 2002. Sonic hedgehog signaling from the urethral epithelium controls external genital development. Dev. Biol. 247, 26–46.
Petiot, A., Perriton, C.L., Dickson, C., Cohn, M.J., 2005. Development of the mammalian urethra is controlled by Fgfr2-IIIb. Development 132, 2441–2450.
Robboy, S.J., Kurita, T., Baskin, L., Cunha, G.R., 2017. New insights insights into human female reproductive tract development. Differentiation 97, 9–22.
Rodriguez, E., Jr., Weiss, D.A., Ferretti, M., Wang, H., Menshenia, J., Risbridger, G., Handelsman, D., Cunha, G., Baskin, L., 2012. Specific morphogenetic events in mouse external genitalia sex differentiation are responsive/dependent upon androgens and/or estrogens. Differentiation 84, 269–279.
Rodriguez, E., Jr., Weiss, D.A., Yang, J.H., Menshenina, J., Ferretti, M., Cunha, T.J., Barcellos, D., Chan, L.Y., Risbridger, G., Cunha, G.R., Baskin, L.S., 2011. New insights on the morphology of adult mouse penis. Biol. Reprod. 85, 1216–1221.
Schlomer, B.J., Feretti, M., Rodriguez, E., Jr., Blaschko, S., Cunha, G., Baskin, L., 2013. Sexual differentiation in the male and female mouse from days 0 to 21: a detailed and novel morphometric description. J. Urol. 190, 1610–1617.
Seifert, A.W., Harfe, B.D., Cohn, M.J., 2008. Cell lineage analysis demonstrates an endodermal origin of the distal urethra and perineum. Dev. Biol. 318, 143–152.
Shah, R.M., Crawford, B.J., 1980. Development of the secondary palate in chick embryo: a light and electron microscopic and histochemical study. Investig. Cell Pathol. 3, 319–328.
Shen, J., Overland, M., Sinclair, A., Cao, M., Yue, X., Cunha, G., Baskin, L., 2016. Complex epithelial remodeling underlie the fusion event in early fetal development of the human penile urethra. Differ.; Res. Biol. Divers. 92, 169–182.
Sinclair, A.W., Cao, M., Baskin, L., Cunha, G.R., 2016a. Diethylstilbestrol-induced mouse hypospadias: "window of susceptibility". Differ.; Res. Biol. Divers. 91, 1–18.
Sinclair, A.W., Cao, M., Shen, J., Cooke, P., Risbridger, G., Baskin, L., Cunha, G.R., 2016b. Mouse hypospadias: a critical examination and definition. Differ.; Res. Biol. Divers. 92, 306–317.
Sun, T.T., Liang, F.X., Wu, X.R., 1999. Uroplakins as markers of urothelial differentiation. Adv. Exp. Med. Biol. 462 (7–18), 103–114, (discussion).
Yang, J.H., Menshenina, J., Cunha, G.R., Place, N., Baskin, L.S., 2010. Morphology of mouse external genitalia: implications for a role of estrogen in sexual dimorphism of the mouse genital tubercle. J. Urol. 184, 1604–1609.
Yucel, S., Liu, W., Cordero, D., Donjacour, A., Cunha, G., Baskin, L.S., 2004. Anatomical studies of the fibroblast growth factor-10 mutant, Sonic Hedge Hog mutant and androgen receptor mutant mouse genital tubercle. Adv. Exp. Med. Biol. 545, 123–148.